APPROVED FOR RELEASE: 2007/02/08: CIA-RDP82-00850R000200040044-7

TEL POLICY,
RESEARCH AND DEVELOPMENT

21 JANUARY 1980 (FOUO 3/80) 1 OF 1

APPROVED FOR RELEASE: 2007/02/08: CIA-RDP82-00850R000200040044-7

APPROVED FOR RELEASE: 2007/02/08: CIA-RDP82-00850R000200040044-7

FOR OFFICIAL USE ONLY

JPRS L/8875

21 January 1980

Worldwide Report

TELECOMMUNICATIONS POLICY, RESEARCH AND DEVELOPMENT

(FOUO 3/80)

FBIS FOREIGN BROADCAST INFORMATION SERVICE

FOR OFFICIAL USE ONLY

APPROVED FOR RELEASE: 2007/02/08: CIA-RDP82-00850R000200040044-7

APPROVED FOR RELEASE: 2007/02/08: CIA-RDP82-00850R000200040044-7

NOTE

JPRS publications contain information primarily from foreign newspapers, periodicals and books, but also from news agency transmissions and broadcasts. Materials from foreign-language sources are translated; those from English-language sources are transcribed or reprinted, with the original phrasing and other characteristics retained.

Headlines, editorial reports, and material enclosed in brackets [] are supplied by JPRS. Processing indicators such as [Text] or [Excerpt] in the first line of each item, or following the last line of a brief, indicate how the original information was processed. Where no processing indicator is given, the information was summarized or extracted.

Unfamiliar names rendered phonetically or transliterated are enclosed in parentheses. Words or names preceded by a question mark and enclosed in parentheses were not clear in the original but have been supplied as appropriate in context. Other unattributed parenthetical notes within the body of an item originate with the source. Times within items are as given by source.

The contents of this publication in no way represent the policies, views or attitudes of the U.S. Government.

For further information on report content call (703) 351-2811.

COPYRIGHT LAWS AND REGULATIONS GOVERNING OWNERSHIP OF MATERIALS REPRODUCED HEREIN REQUIRE THAT DISSEMINATION OF THIS PUBLICATION BE RESTRICTED FOR OFFICIAL USE ONLY.

APPROVED FOR RELEASE: 2007/02/08: CIA-RDP82-00850R000200040044-7

APPROVED FOR RELEASE: 2007/02/08: CIA-RDP82-00850R000200040044-7

JPRS L/8875

21 January 1980

WORLDWIDE REPORT

TELECOMMUNICATIONS POLICY, RESEARCH AND DEVELOPMENT

(FOUO 3/80)

CONTENTS PAGE

WORLDWIDE AFFAIRS

Details of 'SPACECOM' Telecommunications Financing Project
(Pierre Langereux; AIR ET COSMOS, 3 Nov 79) 1

WEST EUROPE

FRANCE

Briefs
New Government Problem 4

ITALY

Synchronous Demodulator for TV Signals Described
(Franco Mussino; ELETTRONICA E TELECOMUNICAZIONI, May-Jun 79) 5

Splicing, Connection Techniques for Optical Fibers
(Feliciano Esposito, Emilio Vezzoni; ELETTRONICA E TELECOMUNICAZIONI, May-Jun 79) 22

USSR

Monitoring Transmission Breaks on Main Coaxial Cables
(N. E. Popova, et al.; ELEKTROSVYAZ', No 10, 1979) 55

Expansion of the Operating Frequency Range of High Capacity Balanced Cables for Analog Transmission Systems
(B. M. Fayerovich, Ye. T. Khvostovitskiy; ELEKTROSVYAZ', No 10, 1979) 62

APPROVED FOR RELEASE: 2007/02/08: CIA-RDP82-00850R000200040044-7

APPROVED FOR RELEASE: 2007/02/08: CIA-RDP82-00850R000200040044-7

WORLDWIDE AFFAIRS

DETAILS OF 'SPACECOM' TELECOMMUNICATIONS FINANCING PROJECT

Paris AIR & COSMOS in French 3 Nov 79 p 31

[Article by Pierre Langereux: "SPACECOM, a Company for Financing Satellites"]

[Text] EUROSPACE, organizer of the "Librespace" [Free Space] Conference held in Paris on 18 and 19 October*, recalled on this occasion, through the words of its secretary general, Yves Demerliac, that it is continuing to promote the SPACECOM project for creation of a company to finance telecommunications and television satellites for the benefit of the countries of Europe and of the Third World.

The SPACECOM project, broached for the first time last year on the occasion of the specialist conferences in Lima, Peru, and Naples, Italy, has been developed by EUROSPACE with the support of the European Space Agency. It is based on the simple observation that there is a large number of countries and organisms capable of using the services provided by the satellites, but that these potential users, taken individually, do not have the means to buy these satellites, which are also becoming increasingly complex, high-performance, and expensive. Moreover, it appears that it could be difficult to set up groups of countries or users for political reasons, for lack of capital, for fear of going into competition with existing organisms (INTELSAT [International Telecommunications Satellite Co] in particular), etc. SPACECOM's mission would therefore be to bring financial means together for purchasing staellites and placing them at the disposal of "authorized" users.

A Considerable Market

The results of an initial investigation conducted by EUROSPACE into the interest in the SPACECOM project on the part of the countries of the Third World were presented to the "Librespace" conference. EUROSPACE contacted 150 P and T [Posts and Telecommunications] organizations in 80 countries, 31 of which were visited. In this way EUROSPACE obtained "54 significant replies, 51 of which express interest in SPACECOM--that is, an intention to participate as investor

* Cf AIR ET COSMOS, No 784.

APPROVED FOR RELEASE: 2007/02/08: CIA-RDP82-00850R000200040044-7

APPROVED FOR RELEASE: 2007/02/08: CIA-RDP82-00850R000200040044-7

and/or user of services." Most of the respondents contacted consider that SPACECOM should in particular make telecommunications systems available to the potential users by the renting of repeaters. But some consider that SPACECOM could also do leasing of ground stations and training of personnel and even offer space teledetection services.

SPACECOM Market Study for 1980 to 1985

Countries contacted in:	"All-purpose" repeaters	Rural repeaters (11-14 GHz)	Direct TV
Black Africa	17	7	2
South America	28	not before 1985	not before 1985
Southeast Asia	24	4	not before 1985
TOTALS:	69	11 +	2 +

It also appears that in the Third World, free enterprise in the area of telecommunications and television will remain timid for a long time to come. Therefore, the only entrepreneurs will remain the ministers of P and T and of information, in the view of EUROSPACE, whose contacts have revealed the existence of a "considerable potential market."

EUROSPACE's study has thus shown that the market for SPACECOM could be estimated at more than 80 repeaters to be leased for the period 1980-1985, on the basis of a very conservatively estimated "rate of capture" of the market (about 30 percent).

SPACECOM must obviously expect to find itself in competition with other companies--the American COMSAT is not unconcerned--and with other national and regional enterprises such as Palapa (Indonesia) and ARABSAT (countries of the Arab League), etc. INTELSAT is also a competitor already established in this market, for the international organization, which today covers 103 countries, presently leases "INTELSAT 5" satellite repeaters to 15 countries, and it is planning to offer more extensive services now to interested countries.

The next generation of satellites of the "Follow-on INTELSAT 5" organization will, furthermore, be designed expressly for offering this service also, in a systematic way, to all interested countries.

For $220 Million

According to the study done by EUROSPACE, SPACECOM should take the form of "nonconventional" commercial company so as to accomodate the special characteristics of telecommunications operations, which generally are government monopolies subject to very strict national and international regulations.

The company could be made up of regional holding companies (for example, for West Africa, the Andean countries, ASEAN [Association of South East Asian

APPROVED FOR RELEASE: 2007/02/08: CIA-RDP82-00850R000200040044-7

APPROVED FOR RELEASE: 2007/02/08: CIA-RDP82-00850R000200040044-7

Nations], etc), whose stockholders would be the "authorized" users (P and T) and other financiers; EUROSPACE is thinking in particular of the holders of petrodollars!

In general, the interlocutors concerned have recognized the interest, indeed the necessity, of accepting, along with SPACECOM's own capital, capital from "outside" that of the operating companies. All have also stressed the necessity of a separation between the utilization and investment sides, and some have even expressed the desire for the control rights of the investors to be limited. The company should also be able to call for loan capital at specail rates, as development aid (COFACE [French Foreign Trade Credit Insurance Company], etc). In toto, SPACECOM's financial needs have been estimated at about $220 million over 10 years to set up an initial regional telecommunications satellite system. This corresponds closely to the startup capital available to the American COMSAT, whose "career"* obviously proves that a lot of money can be made with satellites!

As for the profitability of a company like SPACECOM, it has been estimated at about 15 percent at cruising speed, using European satellites, with privileged access to loans and at repeater leasing rates lower than those of INTELSAT (although the repeaters planned for SPACECOM service have to have higher performance characteristics).

Breaking the Monopolies

According to EUROSPACE, there is already in Europe a sizeable potential body of private entrepreneurs disposed to invest in such a system if they can run it. But at present, the existence of state monopolies means that only "authorized" users could be customers of SPACECOM: that is, either governmental telecommunications or television entities, for whom SPACECOM would simply constitute a "financial relay" (comparable, for example, to FINEXTEL [expansion unknown] in France), or private enterprises such as RTL [expansion unknown], RMC [Radio Monte Carlo], Europe 1, etc, who would not easily find a place on the "national" satellites. SPACECOM could then hope to interest them by offering a collective solution at an affordable price. The company could perhaps also offer new firms an opportunity to get into the market. EUROSPACE notes in this regard that another study, also carried out with the ESA [European Space Agency], "has made it possible to identify an impressive number of credible companies that want to go into pay-television operations and teletext operations" in Europe.

But this obviously presupposes a spectacular new flexibility on the part of the telecommunications and radio and TV-broadcasting and programming monopolies!

When, then, will SPACECOM shares be on the market?

COPYRIGHT: AIR ET COSMOS, Paris 1979

11267
CSO: 5500

APPROVED FOR RELEASE: 2007/02/08: CIA-RDP82-00850R000200040044-7

APPROVED FOR RELEASE: 2007/02/08: CIA-RDP82-00850R000200040044-7

FRANCE

BRIEFS

NEW GOVERNMENT PROBLEM--Concerning the "free" radio broadcast media: Certain employees of the unionized TDF [French (Radio and Television) Broadcasting Service] are refusing to jam the broadcasts of the pirate stations. [Text] [Paris LA LETTRE DE L'EXPANSION in French 24 Dec 79 p 3]

CSO: 5500

APPROVED FOR RELEASE: 2007/02/08: CIA-RDP82-00850R000200040044-7

APPROVED FOR RELEASE: 2007/02/08: CIA-RDP82-00850R000200040044-7

ITALY

SYNCHRONOUS DEMODULATOR FOR TV SIGNALS DESCRIBED

Turin ELETTRONICA E TELECOMUNICAZIONI in Italian May-Jun 79 pp 101-107

[Article* by Franco Mussino, graduate engineer, Electronics and Telecommunications Institute of the Turin Polytechnic]

[Text] Summary [as published]--Synchronous demodulator for television signals. This paper describes a TV demodulator which uses the synchronous detection so that distortions connected to a vestigial signal envelope detection can be eliminated and the overall selectivity of the television receiver improved. Firstly, the i.f. signal is passed through a filter having the same bandwidth of the transmitted signal; then the vision carrier is demodulated both in phase and in quadrature, and the output signals of these demodulators are fed into two all-pass networks having a constant phase difference of 90°. The outputs of these two all-pass networks are combined in such a way that the components belonging to the full r.f. sideband are added in phase, while those belonging to the vestigial r.f. sideband cancel each other. The resulting amplitude response is constant over the whole video band and the selectivity is better than that achieved with conventional demodulators.

1. Introduction

The demodulation of the television signal is one of the essential functions of the television receiver and has undergone considerable development over the years to improve it.

From the beginning of television until a few years ago, envelope detection was universally used both in black-and-white and in color receivers to demodulate the luminance component. Synchronous detection was used in color television receivers only to demodulate the chrominance component.

---

* [Editor's note] Typewritten manuscript received 18 May 1979.

APPROVED FOR RELEASE: 2007/02/08: CIA-RDP82-00850R000200040044-7

APPROVED FOR RELEASE: 2007/02/08: CIA-RDP82-00850R000200040044-7

More recently, the introduction of integrated circuits has made possible (from an economy viewpoint) the use of synchronous detection for the luminance component as well. The synchronous demodulator is in fact more complex than the envelope detector and hence more costly, but it has the advantage of being able to eliminate the quadrature distortions present in the television signal envelope as a result of the partial suppression of the lower sideband.

In effect, the synchronous demodulators in use today in television receivers (for example, the Philips TBA 440 and other manufacturers' similar products cannot, strictly speaking, be considered as such (they are in fact pseudo-synchronous), in that the video carrier is reconstituted by filtering and amplitude-limiting the received television signal, so that the carrier's phase modulations (produced by the partial suppression of the sideband) act upon the instantaneous phase of the reconstituted video carrier in the receiver and therefore upon the resultant demodulation itself.

The major culprit responsible for such phase modulations at low frequencies[1] is the intermediate-frequency filter, which attenuates asymmetrically the video carrier sidebands (Nyquist slope) (see Figure 1).

Key:

1. Adjacent channels
2. Sound carrier
3. Color subcarrier
4. Video carrier

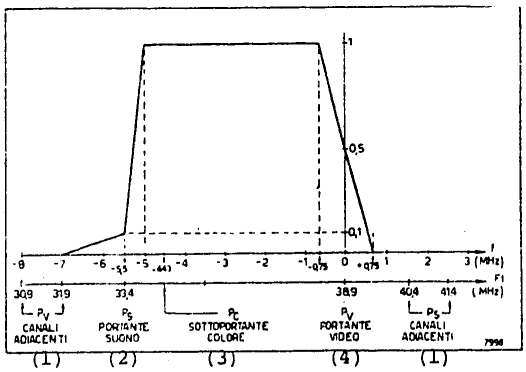

Fig 1 - Ideal amplitude response curve of I.F. filter with Nyquist slope.

To reduce such phase modulation of the reconstituted video carrier as much as possible, the passband of the filter used to extract the carrier must be made as narrow as possible within the constraints imposed by the required sharpness of tuning and its long-term stability. The passband of this filter can be substantially reduced by using frequency synthesizer tuners; often,

APPROVED FOR RELEASE: 2007/02/08: CIA-RDP82-00850R000200040044-7

APPROVED FOR RELEASE: 2007/02/08: CIA-RDP82-00850R000200040044-7

however, the received signals are not of the required frequency precision and stability, as occurs, for example, when frequency conversions have been introduced in the central antenna network, and for this reason a sufficiently broad tuning band must be provided.

It follows from all these considerations that for effective synchronous demodulation, the video carrier must be reconstituted not by filtering and amplitude-limiting, but rather by using an oscillator synchronized in phase with the video carrier itself (see Figure 2). The low-pass filter present in the loop of the in-phase locking circuit (PLL: phase-locked loop) must be designed to eliminate from the VCO control voltage the frequencies involved in the phase modulation of the video carrier, thus obtaining a signal free of spurious phase modulations, to which true synchronous modulation can be applied.

Key:

1. Multiplier
2. Voltage-controlled oscillator
3. Low-pass filter

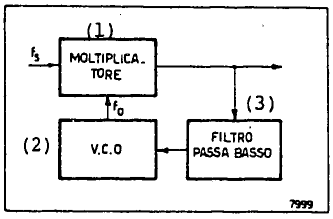

Fig 2 - Block diagram of a PLL circuit for synchronizing the oscillator frequency f_o with the incoming signal frequency f_s.

The purpose of this paper is to describe a method whereby the performance characteristics of a television demodulator can be further improved, still using synchronous demodulation but in a different context,[2] that is, using an intermediate-frequency filter with a broad enough bandwidth to present to the demodulator the entire received signal without alterations to its spectrum, thus avoiding the generation of low-frequency components by way of phase modulation of the video carrier and considerably facilitating its reconstitution, even when a PLL circuit (Figure 2) is used.

The shape of the ideal amplitude response curve of a filter meeting the above requirements is shown in Figure 3. In practice, this curve coincides with saturation masking for modulation of the television transmitter (CIRR television systems B and G).

APPROVED FOR RELEASE: 2007/02/08: CIA-RDP82-00850R000200040044-7

APPROVED FOR RELEASE: 2007/02/08: CIA-RDP82-00850R000200040044-7

Key:

1. Adjacent channels
2. Sound carrier
3. Color subcarrier
4. Video subcarrier

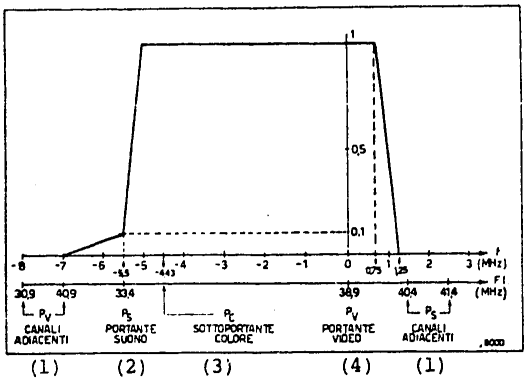

Fig 3 - Ideal amplitude response curve of I.F. filter for the demodulator described herein.

2. Block Diagram of Television Demodulator

The demodulator itself (Figure 4) consists of two synchronous detectors, one of which operates in phase with the video carrier and the other in quadrature with the same carrier.

Key:

1. Local oscillator
2. R.F. amplifier and converter
3. I.F. amplifier
4. In-phase synchronous detector
5. Low-pass filter
6. Phase-shift network
7. Combiner
8. Video amplifier
9. Synchronixed oscillator
10. Synchronous detector in quadrature

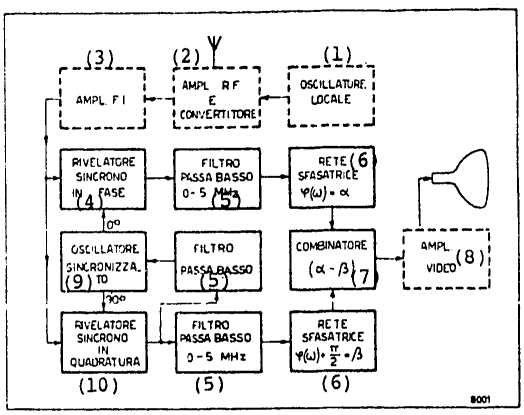

Fig 4 - Block diagram of synchronous demodulator for TV signals, with R.F., I.F. and video frequency stages of receiver shown dotted.

APPROVED FOR RELEASE: 2007/02/08: CIA-RDP82-00850R000200040044-7

APPROVED FOR RELEASE: 2007/02/08: CIA-RDP82-00850R000200040044-7

Figures 5 and 6 show that in the frequency band in which both sidebands of the received television signal are present, an output is obtained only from the synchronous detector operating in phase with the video carrier, the output from the synchronous detector operating in quadrature with the carrier being zero. On the other hand, in the frequency band containing only one of the sidebands, an output is obtained from both the detectors, whose amplitude, however, is only half that of the preceding case. Since these two outputs are equal to each other in amplitude but 90° out of phase with each other, this phase difference can be transformed in such a way that the signals from the two demodulators will arrive at the combiner input (Figure 4) in phase if they originated in the desired sideband, or 180° out of phase if they originated in the other sideband. This is the system used also in audio receivers to demodulate SSB (single sideband) transmissions by the so-called phase-detection method.

In the television case, however, there is the advantage that the constant 90° phase difference required between the outputs of the two phase-shift networks is needed only within the frequency range in which only one of the sidebands is transmitted (750 kHz-5 mHz), that is, over less than a decade. This simplifies considerably the design and construction of the phase-shift network.[3]

As regards selectivity, the demodulation method described above (Figure 4) permits a decided reduction in interference from the lower television channel. In fact,[2,3] the unwanted sideband suppression S (in dB) depends on the phase displacement φ with respect to 90° introduced by the phase-shift network:

$$S = 20 \log_{10} \frac{1}{\mathrm{tg}(\varphi/2)} . \qquad (1)$$

With values of φ not exceeding $\pm 2^{\circ}$, it is possible to obtain an unwanted-sideband suppression of not less than 35 dB.

Moreover, the overall selectivity can be further increased with respect to that introduced by the I.F. filter, by means of video frequency low-pass filters, placed, that is, after the synchronous detectors (see Figure 4).

Regarding the signal/noise ratio obtainable with the demodulator described herein, it can be quickly stated that it is practically no different from that obtainable with a conventional type of demodulator (synchronous or envelope, placed after the I.F. filter with Nyquist slope), at least as long as the signal-to-noise ratio is sufficiently high, as is normally the case.

APPROVED FOR RELEASE: 2007/02/08: CIA-RDP82-00850R000200040044-7

APPROVED FOR RELEASE: 2007/02/08: CIA-RDP82-00850R000200040044-7

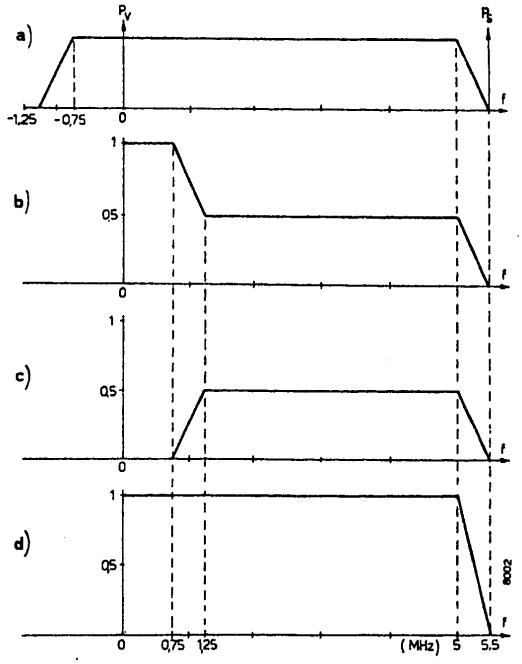

Fig 5 - Amplitude curves of:

a) transmitted TV signal

b) output signal from the synchronous detector in phase with the carrier

c) output signal from the synchronous detector in quadrature with the carrier

d) total output signal

APPROVED FOR RELEASE: 2007/02/08: CIA-RDP82-00850R000200040044-7

APPROVED FOR RELEASE: 2007/02/08: CIA-RDP82-00850R000200040044-7

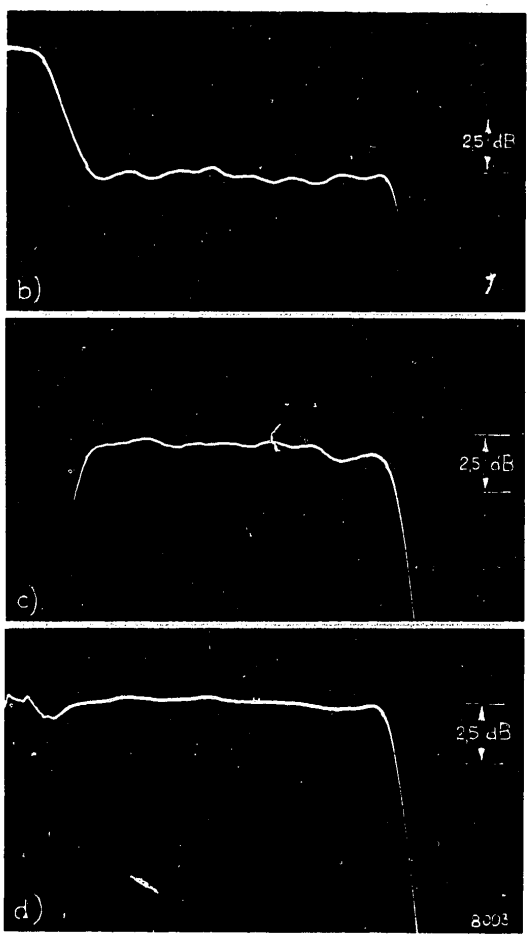

Fig 6 - Response curves obtained experimentally, corresponding to curves b), c), d) of Fig 5.

APPROVED FOR RELEASE: 2007/02/08: CIA-RDP82-00850R000200040044-7

APPROVED FOR RELEASE: 2007/02/08: CIA-RDP82-00850R000200040044-7

For a conventional type demodulator (preceded by the I.F. filter with Nyquist slope), the signal-to-noise ratio S/N* at the output of the demodulator is linked to the carrier-to-noise ratio C/N** prior to demodulation, by the relation (see Appendix):

$$(S/N)_{dB} = (C/N)_{dB} - 7 \text{ dB}. \qquad (2)$$

In such case, the equivalent noise bandwidth (with filter with Nyquist slope) is 4.75 MHz.

For the demodulator of Figure 4 (preceded by the I.F. filter of Figure 3), the link between S/N and C/N is still expressed by the above relation, while the equivalent noise bandwidth is 5 MHz (see Appendix).

3. Description of Circuit

Figure 7 shows a functional diagram of the I.F. amplifier and the in-phase and in-quadrature synchronous demodulators. Figure 8 shows the 90° broadband phase-shift circuit, the combining circuit and the video amplifier.

The circuits shown in Figures 7 and 8 are mounted separately, each on a printed circuit board.

As indicated in Figure 7, I.F. amplifier A_1 consists of an integrated circuit equipped with AGC [automatic gain control].

The I.F. filter (described further on) that precedes amplifier A_1 is mounted on a suitable printed circuit board (Figure 9), which can be substituted by another card (Figure 10) containing also the converter circuits for the VHF and UHF bands. This makes it possible to use the demodulator both when the television signal is at the intermediate frequency and when it is at radio frequency (VHF and UHF bands).

$$* \ (S/N)_{dB} = 20 \log_{10} \frac{\text{peak-to-peak amplitude of video signal (black-and-white transmission)}}{\text{effective value of unweighted noise}}$$

$$** \ (C/N)_{dB} = 20 \log_{10} \frac{\text{effective value of video carrier during synchronizing pulses}}{\text{effective value of noise at radio frequency}}$$

APPROVED FOR RELEASE: 2007/02/08: CIA-RDP82-00850R000200040044-7

APPROVED FOR RELEASE: 2007/02/08: CIA-RDP82-00850R000200040044-7

The output of the I.F. amplifier drives directly the two multipliers M_1 and M_2 (Figure 7) , which also receive the signals from the VCO operating at a frequency of 38.9 MHz. The VCO drives the 90° phase-shift network through which the oscillator's signal is fed to the two multipliers. The amplitude and relative phase of the VCO output signals are adjustable by means of P_2 and P_1 respectively.

The multiplier output signals are filtered by pi-type LC low-pass filters (described below) and amplified in A_2 and A_3 by about 100 volts.

Potentiometers P_3 and P_4 are used to balance the output levels of differential amplifiers A_2 and A_3 in the absence of a signal. Balance is indicated by meters S_1 and S_2 shown in Figure 7, which are mounted on the front panel and connected between the outputs of each of the two differential amplifiers. These meters also furnish useful indications of the demodulator signal intensity (S_1) as well as of the exact tuning of the converter circuit and of the VCO (S_2).

Since the output signals from A_2 and A_3 have different direct current components (as will be explained further on) they must be put through an equalizing circuit before being sent to the 90° broadband phase-shift networks and to the combiner circuit. The D.C. component is restored by means of a suitable circuit (see Figure 7) and made equal for both channels (the in-phase and the in-quadrature), while amplifiers A_4 and A_5 provide the 50-ohm output impedance required to drive the phase-shift networks.*

The output of A_2 is also used to obtain the AGC signal for I.F. amplifier A_1 and for the tuners, and that of A_3 to obtain the automatic frequency control [AFC] signal for the VCO and the tuner circuits.

In fact, the output of the demodulator that is in phase with the carrier contains a D.C. component of the same amplitude as the carrier, whereas that of the demodulator in quadrature has a zero D.C. component if the phase difference between the VCO signal and the signal representing the carrier is exactly 90°. If it is not, there will be a D.C. component proportional in amplitude and sign to the variance of the phase difference from the 90° condition. This signal is amplified by about 10 volts through A_6, and is used to control the VCO frequency. This signal is also used through A_9 to control the tuning frequency of the varactor-equipped tuning circuit (Figure 7). Potentiometer P_5 permits tuning the R.F. signal when the card containing the VHF and UHF tuning circuits is used (Figure 10). Potentiometer P_5 is in fact associated with a push-button switch panel that permits selection of the desired tuning band (bands I, III, IV and V) as well as presetting of one channel for each of the mentioned bands.

---

* This value of impedance was selected to facilitate measurements on the phase-shift network by means of the network analyzer.

APPROVED FOR RELEASE: 2007/02/08: CIA-RDP82-00850R000200040044-7

APPROVED FOR RELEASE: 2007/02/08: CIA-RDP82-00850R000200040044-7

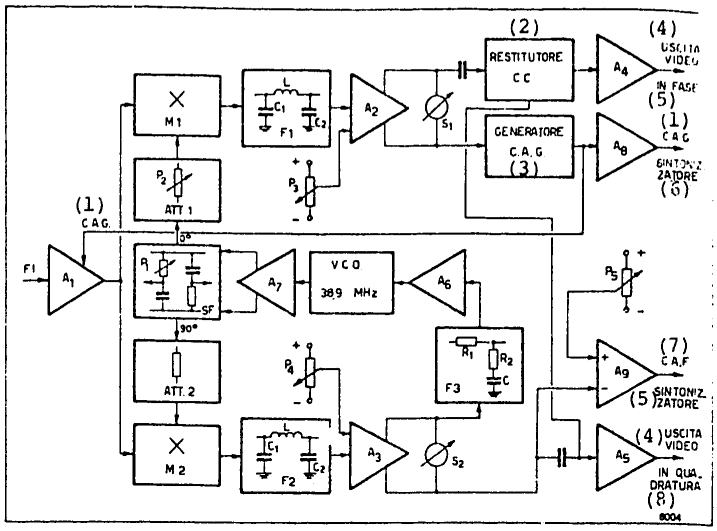

Fig 7 - Functional block diagram of synchronous demodulator.

Key:

1. Automatic gain control (AGC)
2. D.C. restorer
3. AGC generator
4. Video output
5. In phase
6. Tuner
7. Automatic frequency control (AFC)
8. In quadrature

APPROVED FOR RELEASE: 2007/02/08: CIA-RDP82-00850R000200040044-7

APPROVED FOR RELEASE: 2007/02/08: CIA-RDP82-00850R000200040044-7

Key:

1. Video output
2. In phase
3. In quadrature
4. Combiner
5. Video amplifiet
6. Video output

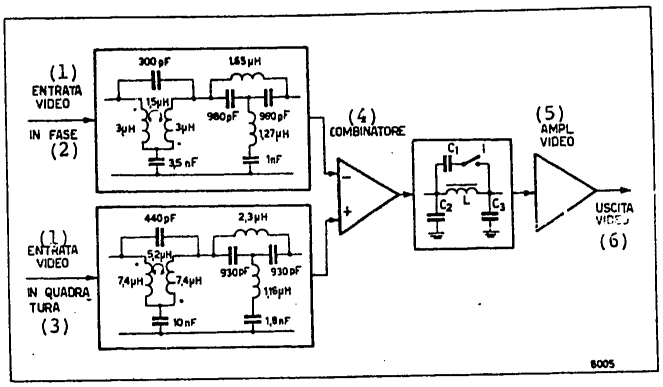

Fig 8 - Diagram of broadband 90° phase-shift networks of the combiner, video amplifier and low-pass filter with 5.5-MHz trap (plug-in) circuits. The broadband 90° phase-shift networks require 50-ohm generator and load impedances.

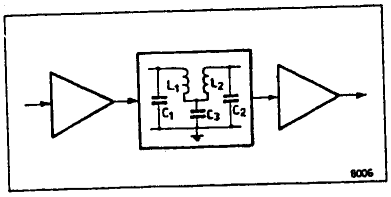

Fig 9 - I.F. filter with separate input and output stages.

Key:

1. Mixer
2. VHF tuner
3. UHF tuner
4. Automatic frequency control (AFC)
5. Automatic gain control (AGC)

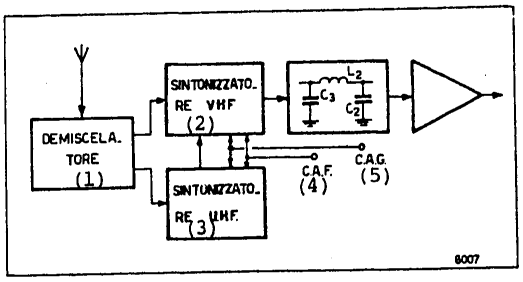

Fig 10 - I.F. filter and tuning circuit for VHF and UHF bands.

APPROVED FOR RELEASE: 2007/02/08: CIA-RDP82-00850R000200040044-7

APPROVED FOR RELEASE: 2007/02/08: CIA-RDP82-00850R000200040044-7

Figure 8 shows the 90° broadband phase-shift networks[3], by means of which a 90° phase difference (constant within $\pm 2^{\circ}$) is obtained in the band of frequencies between 1.25 MHz and 5 MHz (Figure 11).

Moreover, the phase-shift network to which the signal is fed from the output of the demodulator that is in phase with the video carrier is designed to introduce a delay ($\cong 0.2 \mu s$), constant within the video band, as required to avoid distortion of the television signal.

The signals from the outputs of the phase-shift networks are fed to a differential amplifier (Figure 8) and successively, through a low-pass filter which also introduces a substantial attenuation of the sound carrier at the 5.5 MHz frequency, to a video amplifier capable of delivering an output signal of 1 V_{pp} across a suitable 75-ohm load.

4. Design Criteria

The basic design criteria used are briefly set forth here for some parts of the circuit and principally the filters, both for the television signal (at I.F. and at video frequency) and for the PLL.

The I.F. filter consists simply of a double-tuned circuit (Figure 9) critical-coupled through condenser C_3. The attenuation of this filter at the sound carrier frequency (33.4 MHz) is rather minor, but owing to the linearity of the circuits following it no intermodulation problems were encountered.

The LC π low-pass filters that follow the multipliers (Figure 7) were designed for optimum compromise between phase-response linearity and attenuation of frequencies beyond 5 mHz. A Legendre-Thomson filter[4] was adopted, with $m = 0.6$ and $f_{3dB} = 11$ MHz. The values obtained for generator and load impedances of 500 ohms* are: $L = 8.2\ \mu H$, $C_1 = 14$ pF, $C_2 = 64$ pF.

The low-pass filter that follows the combiner circuit was designed for high attenuation ($\cong 50$ dB) of the sound carrier at 5.5 MHz. An m-derived filter design was therefore adopted with cutoff frequency $f_{3dB} = 5.2$ MHz and infinity attenuation frequency $f_{\infty} = 5.5$ MHz.
tor and load impedances of 500 ohms are: $L = 10 \mu H$, $C_1 = 84$pF, $C_2 = C_3 = 20$ pF. Taking capacitor C_1 out of the circuit by means of switch I (see Figure 8), we obtain a Butterworth filter with cutoff frequency at 16 MHz, which therefore introduces negligible attenuation to a frequency of 5 MHz. This capability is especially useful when the demodulator is used to effect measurements on generators of television signals, from which it is possible to exclude the sound carrier.

---

* This impedance value was chosen based on circuit requirements.

APPROVED FOR RELEASE: 2007/02/08: CIA-RDP82-00850R000200040044-7

APPROVED FOR RELEASE: 2007/02/08: CIA-RDP82-00850R000200040044-7

The low-pass filter F_3 (see Figure 7 of the phase-locked loop (PLL) consists of resistors R_1, R_2 and capacitor C. The values chosen ($R_1 = 4.7$k ohms, $R_2 = 82$ ohms, $C = 2\mu f$) provide a low enough cutoff frequency together with a fast locking-in time.

The lock-in holding interval is ± 1.5 MHz with an input voltage of approximately 3 mV to the amplifiers. This interval diminishes proportionally with lower voltage input values. The locking-in time with the above input voltage is approximately ± 300 kHz.

5. Experimental Results

To verify experimentally the performance of the above-described demodulator, test measurements were run on some of the more significant values.

As regards the baseband signal-to-noise ratio, understood as the ratio between the useful signal amplitude (transition between white and black levels) and the effective noise (unweighted) value, a determination of S/N = 44 dB was obtained with a 1 mV radio-frequency (VHF) input signal (corresponding to a ratio C/N of approximately 60 dB). From these values and relation (1), the noise figure obtained(predominantly owing to the converter) is approximately 11 dB.

Moreover, using comparative measurements, the attenuation of the adjacent lower sideband was found to be 20-25 dB greater than that obtainable with a conventional type demodulator.

To test the linearity of the amplifier circuits used, the differential gain and differential phase were measured at their outputs and found to be less than 3 percent and 4° respectively; moreover, the chrominance-luminance gain inequality was found to be less than 1 dB, and their delay inequality 50 nanoseconds.

6. Conclusions

A television signal demodulator has been described that utilizes synchronous detection in a different manner from demodulators currently available on the market.

This synchronous demodulator has been designed in such a manner as to not only reduce the distortion inherent in the envelope demodulators widely used until now, but also to obtain an improvement in performance characteristics as compared with those of pseudosynchronous demodulators, by eliminating the spurious phase modulations owing to the intermediate-frequency filter and the manner used to reconstitute the carrier. The overall receiver selectivity is also improved, especially as regards the lower adjacent channel. The use of SAW (surface acoustic wave) filters having the amplitude response curves shown in Figure 3 would further increase the

APPROVED FOR RELEASE: 2007/02/08: CIA-RDP82-00850R000200040044-7

APPROVED FOR RELEASE: 2007/02/08: CIA-RDP82-00850R000200040044-7

receiver selectivity without reducing the demodulated signal bandwidth. This is an increasingly important characteristic, owing to the congestion on the television broadcast band and to plans for new services such as Teletext, which is especially subject to degradation from interfering signals.

Warmest thanks are hereby extended to Prof Mario Pent for his thorough review of this manuscript.

Turin, Istituto Elettrotecnico Nazionale Galileo Ferraris.

Appendix

The statement of the relation that expresses the ratio between signal and noise (S/N) in the baseband, and the ratio between carrier and noise (C/N) at intermediate frequency (prior to the demodulator) is based on the following considerations.

If n is the spectral density of the noise amplitude at intermediate frequency prior to the demodulator, the corresponding noise voltage N is given by:

$$N = n\sqrt{B_{eq}}, \tag{3}$$

where B_{eq} represents the equivalent bandwidth of overall noise of the receiver (in practice, it is given as that of the intermediate-frequency filter) and is defined as:

$$B_{eq} = \frac{1}{|A_{vo}|^2} \int_{-\infty}^{+\infty} |A_v(f)|^2 \, df \quad , \tag{4}$$

where the function $|A_v(f)|$ describes the shape of the amplitude response curve and A_{vo} represents the maximum value of that curve. With an intermediate-frequency filter with Nyquist slope (Figure 1):

$$B_{eq} = \frac{1}{|A_{vo}|^2} \int_{-0.75\ \mathrm{MHz}}^{+5\ \mathrm{MHz}} |A_v(f)|^2 \, df = \tag{5}$$

$$= \frac{1}{|A_{vo}|^2} \left[\int_{-0.75\ \mathrm{MHz}}^{+0.75\ \mathrm{MHz}} \left| A_{vo} \frac{f + 0.75}{1.5} \right|^2 df + \right.$$

$$\left. + \int_{+0.75\ \mathrm{MHz}}^{+5\ \mathrm{MHz}} |A_{vo}|^2 \, df \right] = 0.5 + 4.25 = 4.75\ \mathrm{MHz}$$

APPROVED FOR RELEASE: 2007/02/08: CIA-RDP82-00850R000200040044-7

APPROVED FOR RELEASE: 2007/02/08: CIA-RDP82-00850R000200040044-7

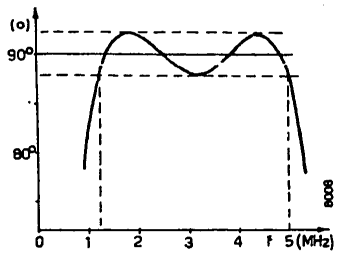

Fig 11 - Curve of phase difference between outputs of the two phase-shift networks of Figure 8 as a function of frequency.

Key:

1. Black level
2. White level

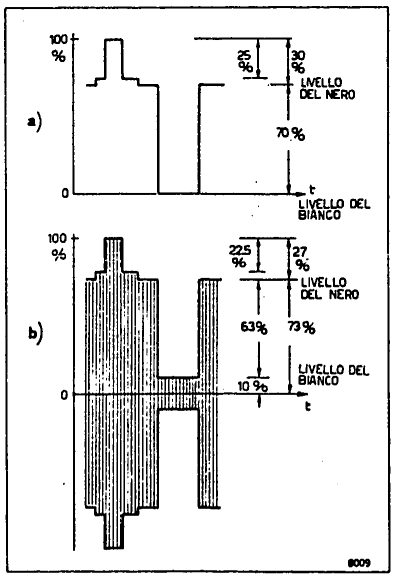

Fig 12 - Relative levels of television signal at baseband (a) and at radio frequency (b).

APPROVED FOR RELEASE: 2007/02/08: CIA-RDP82-00850R000200040044-7

APPROVED FOR RELEASE: 2007/02/08: CIA-RDP82-00850R000200040044-7

Noise at frequencies beyond 5 mHz is disregarded, inasmuch as it will be attenuated later by the base band filters as well.

The noise value obtained after the demodulator is, in this case, still expressed by relation (3).

To calculate the ratio between the effective value C of the video carrier during synchronizing pulses and the amplitude S of the video signal(transition between black and white levels), it should be noted that, after the intermediate-frequency filter with Nyquist slope (Figure 1), the amplitude V of the video carrier is halved, so that:

$$V = \frac{C}{2}\sqrt{2} \ . \tag{6}$$

The amplitude S of the white-black transition in the baseband, however, assuming an ideal detector, is related to the amplitude V of the video carrier before demodulation by:

$$S = mV \tag{7}$$

where m represents the depth of modulation relative to white-black transition. Hence the relation between C/N and S/N is:

$$\frac{C}{N} = \frac{S}{N}\,\frac{\sqrt{2}}{m} \ . \tag{8}$$

For B and G television systems, $m = 0.63$ (Figure 12); in terms of logarithmic units (dB), we obtain:

$$\left(\frac{C}{N}\right)_{dB} = \left(\frac{S}{N}\right)_{dB} + 7.023 \text{ dB} \ . \tag{9}$$

In the case in which the intermediate-frequency filter has a response curve like the one shown in Figure 3 and the demodulator is the one indicated in Figure 4, the amplitude S of the video signal (transition between white and black levels) is double that of the preceding case, since the video carrier is not attenuated and the amplitude of the modulating signal is reconstituted by adding the outputs of the two demodulators across the phase-shift networks (Figures 4 and 5). Hence:

$$S = mC\sqrt{2} \ . \tag{10}$$

With regard to noise, it must be considered that the components having frequencies less than 0.75 MHz are present in both the sidebands and result in contributions whose powers are added at the output of each demodulator; the

APPROVED FOR RELEASE: 2007/02/08: CIA-RDP82-00850R000200040044-7

APPROVED FOR RELEASE: 2007/02/08: CIA-RDP82-00850R000200040044-7

contributions of each of the two demodulators in turn also add their powers, since at those frequencies the relative phase shift introduced by the phase-shift networks is much less than 90°. Hence, P_{N1} being the noise power contribution by each sideband, the output noise power P_N is:

$$P_N = 4\,P_{N1}\ . \tag{11}$$

For components having a frequency higher than 0.75 mHz, on the other hand, the noise contributions come from only one sideband, but they voltage-add, since they are combined in phase by the action of the phase-shift networks. Therefore, in this case as well, the preceding relation is valid.

The result, therefore, is that not only signal S but also noise voltage N double with respect to the case of the demodulator preceded by an intermediate-frequency filter with Nyquist slope, and hence the foregoing relation between S/N and C/N is also still valid.

The equivalent noise bandwidth in this case is 5 mHz, since no bandwidth limitation is introduced by the intermediate frequency filter.

BIBLIOGRAPHY

1. Rzeszewski, Ted: "A System Approach to Synchronous Detection," IEEE TRANSACTIONS ON CONSUMER ELECTRONICS, May 1976.

2. Mussino, F.: "Ricevitori con rivelazione coerente per radiodiffusione sonora e televisiva" [Receivers with Coherent Detection for Sound and Television Broadcasting], ELETTRONICA E TELECOMUNICAZIONI no. 2, March-April 1971.

3. Beccari, C., Mussino, F.: "Reti passatutto con differenza di fase costante" [All-pass Filters with Constant Phase difference], ELETTRONICA E TELECOMUNICAZIONI no. 3, 1976.

4. Aiello, G.L., Angelo. P.M.: "Transitional Legendre-Thomson Filters'" IEEE TRANSACTIONS ON CIRCUITS AND SYSTEMS, January 1974, pp 159-162.

COPYRIGHT: 1974 BY ERI-EDIZIONI RAI RADIOTELEVISIONE ITALIANA

9399

CSO: 5500

APPROVED FOR RELEASE: 2007/02/08: CIA-RDP82-00850R000200040044-7

APPROVED FOR RELEASE: 2007/02/08: CIA-RDP82-00850R000200040044-7

ITALY

SPLICING, CONNECTION TECHNIQUES FOR OPTICAL FIBERS

Turin ELETTRONICA E TELECOMUNICAZIONI in Italian May-Jun 79 pp 109-120

[Article* by Feliciano Esposito and Emilio Vezzoni, graduate engineers, Telecommunications Research and Study Center, Turin: "Splicing and Connection Techniques for Optical Fibers"]

[Text] Summary [as published].--Splicing and connection techniques for optical fibres.--We illustrate the main parameters defining the coupling of two optical fibres underlining the effects of positioning errors on coupling losses. Afterwards, we examine the different technologies used for permanent splicings (fusion, sleeve, groove splices) in particular for single fibre and multifibre cables pointing out the main characteristics. The most important demontable connectors (i.e. connectors using watch-jewels, grooves, molding techniques, concentric or eccentric cylinders or beam expansion) are then described together with the main data. These characteristics should allow the detection of the best permanent splice or connector meeting particular requirements.

1. Introduction

The techniques and available means for jointing fiber-optics cables of the single-fiber or the multifiber types fall into either of two basic categories determined by two alternative forms of service criteria.

In the one case, a permanent connection is required; for example, and principally, when section lengths must be jointed to make up a complete system length.

In the other case, the requirement is for a connector that can be joined to or disjoined from its counterpart to make or unmake a junction between, for example, two single optical fibers or two multifiber cables,

* [Editor's note] Typewritten manuscript received 2 May 1979.

APPROVED FOR RELEASE: 2007/02/08: CIA-RDP82-00850R000200040044-7

APPROVED FOR RELEASE: 2007/02/08: CIA-RDP82-00850R000200040044-7

or between a light source and a fiber, or between a detector and a fiber. This requirement generally prevails at the interface between the optical-fiber cable and the transmitter-receiver terminals of the system.

Both cases demand maximum transfer of light power between the two fibers, or between the fiber and the electro-optical component, being jointed. The insertion loss of the joint must therefore be held within strict limits. This total insertion loss can be made up of losses in two categories: a) intrinsic losses, and b) extrinsic losses.

The first of these depend upon the characteristics of the two optical fibers at the point of connection, whereas those in the second category have their origin in the physical imperfections of the joint.

The following parameters are among the most important ones affecting intrinsic losses in the joint between two optical fibers: the difference between their core diameters, the difference between their maximum refractive indexes (and hence their numerical apertures), and the difference between their refractive-index profiles.

These types of losses can play a significant role when it has not been possible to preselect the optical fibers that are to be interconnected. In practice, they can be reduced only by accurately controlling the homogeneity of the fiber during production.

In characterizing a joint it is therefore necessary to determine the full extent to which these losses make up the total insertion loss.

We define the extrinsic losses as those attributable to the following factors: axial offset, axial separation and angular misalinement of the ends of the two coupled optical fibers (in other words, errors in mutual positioning of the ends); variations in the two surfaces (with respect to the ideal condition that they should be specular, plane and orthogonal with their own axes), in other words: non-orthogonality, roughness, non-planarity.

The losses examined herein were evaluated by means of various theoretical models, and found to conform in varying degrees with experimental results.

The more simplified theories assume that the distribution of the optical power among the modes of the fibers is uniform,[1 2 3 4] thus neglecting the coupling between modes and the differences that exist between them as regards excitation and attenuation. More refined approaches take into account the dispersion effects that lead to the stationary-state distribution,[5] or provide a phenomenological model which, though theoretically not rigorous, leads to accurate results.[6]

APPROVED FOR RELEASE: 2007/02/08: CIA-RDP82-00850R000200040044-7

APPROVED FOR RELEASE: 2007/02/08: CIA-RDP82-00850R000200040044-7

Since the purpose of this paper is to summarize the technologies being used to effect the coupling, we limit ourselves to reviewing a few simplified expressions from bibliographical reference 7 for the losses produced as a result of errors in the mutual positioning of the two fibers at the point of junction. These expressions provide a simple means of calculating the mechanical tolerances required of joints.

We point out that these expressions are valid only in the case of coupling between two multimode optical fibers of low light-guiding efficiency and equal to each other, that they assume uniform optical power distribution among the modes, which appears to be the most critical condition, and that they therefore impose more stringent design criteria.

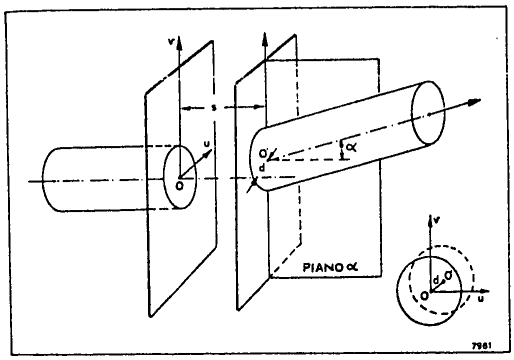

Fig 1 - Degrees of freedom in coupling of two optical fibers.

Referring to Figure 1, the mutual positioning errors between the ends of the two fibers being coupled are indicated as follows:

s = separation error,

α = angular misalinement error,

d = axial offset error,

u = component of d along axis of rotation of angular misalinement α,

$v = \sqrt{d^2 - u^2}$.

The other symbols used are:

a = core radius,

Δ = axial numerical aperture of the optical fiber,

n = refractive index of the intervening medium,

APPROVED FOR RELEASE: 2007/02/08: CIA-RDP82-00850R000200040044-7

APPROVED FOR RELEASE: 2007/02/08: CIA-RDP82-00850R000200040044-7

$\bar{s} = (s/a) \cdot (\Delta/\sqrt{n^2 - \Delta^2})$ = normalized separation,

$\bar{\alpha} = n \sin\alpha/\Delta$ = normalized misalinement,

$\bar{d} = d/a$ = normalized offset,

$\bar{u} = u/a$, $\bar{v} = v/a$ = normalized component of d,

$\bar{e}$ = normalized generic error (any one, among $\bar{s}$, $\bar{u}$, $\bar{v}$, $\bar{\alpha}$) .

We define positioning loss as:

$$L = 10 \log \frac{W_M}{W(u, v, s, \alpha)} \tag{1}$$

where $W(u, v, s, \alpha)$ is the actual value of power measured at the output of the fiber that is at the downstream end of the joint, and W_M is the value corresponding to optimum positioning.

L takes into account only the losses owing to s, α, u, v, that is, of the losses owing to an error with respect to optimal positioning, and neglects Fresnel losses, losses owing to poor quality of terminations and intrinsic losses.

Limiting ourselves to the case of small coupling errors ($\bar{e} \ll 1$), which is in any case a requirement for a high-efficiency joint, the loss owing to a single error is given by:

$$L(\bar{e}) = k\bar{e} \tag{2}$$

where k is a suitable constant (see Table A).

Table A

Coefficient k

$\bar{e}$	parabolic graded-index profile	step-graded profile
$\bar{s}$	2.17	1.84
$\bar{d}$	3.69	2.76
$\bar{\alpha}$	3.69	2.76

The law of compounding errors by twos is expressed by :

$$L^m(\bar{e}_1, \bar{e}_2) = L^m(\bar{e}_1) + L^m(\bar{e}_2) \tag{3}$$

APPROVED FOR RELEASE: 2007/02/08: CIA-RDP82-00850R000200040044-7

APPROVED FOR RELEASE: 2007/02/08: CIA-RDP82-00850R000200040044-7

where $\bar{e}_1$, $\bar{e}_2$ is any arbitrary pair of errors, and the values of m are furnished by Table B.

Table B
Exponent m

$e_1 - e_2$	parabolic graded-index profile	step-graded profile
$s - \alpha$	2	1
$s - u$ $(s - d)$	2.55	2.52
$u - \alpha$	2	1

When all errors are present simultaneously, a general expression can be used, which is obtained from a numerical approximation:

$$(4) \qquad L(\bar{s}, \bar{u}, \bar{v}, \bar{\alpha}) = \left[L^2(\bar{s}) + L^2(\bar{d}) + L^2(\bar{\alpha}) + - c_1 \cdot L(\bar{s}) \cdot L)\bar{d}) + c_2 (L(\bar{s}) + L(\bar{d})) \cdot L(\bar{\alpha}) + + c_3 \cdot L(\bar{s}) \cdot L(\bar{v}) \cdot L(\bar{\alpha})\right]^{1/2} .$$

Coefficients c_i are given in Table C.

Table C
Coefficient c

c	parabolic graded-index profile	step-graded profile
c_1	0.24	0.23
c_2	0	2
c_3	0.46	0.54

We emphasize again that (2), (3) and (4) are approximate expressions and that, besides, (3) and (4) are derived from closer numerical approximations; they nevertheless permit a simple evaluation of the upper limit of the losses owing to a single error or the compounding of several errors.

APPROVED FOR RELEASE: 2007/02/08: CIA-RDP82-00850R000200040044-7

APPROVED FOR RELEASE: 2007/02/08: CIA-RDP82-00850R000200040044-7

From the experimental viewpoint, many results have been included, even though not always homogeneous among themselves owing to the diverse experimental conditions involved.

With regard to a correct evaluation of the influence exerted by geometrical errors in the mutual positioning of two optical fibers, various researchers have carried out measurements designed to evaluate coupled power as a function of such errors. To this end, a method has been adopted that makes it possible to distinguish between the extrinsic and intrinsic loss components. This is done by coupling the two ends obtained by a single cut through a single optical fiber, taking special precautions to avoid any relative rotation between the two ends about the axis of the coupled fibers, and thus assuring the coupling of two ends with identical optical and geometrical characteristics.

The extrinsic losses thus isolated consist of losses by reflection and losses owing to the quality of the ends and their positioning. The two latter ones, defined in relation (1), can be isolated from the first by using an apparatus that makes it possible to obtain the angular misalinement α and the linear offsets u, v, and s indicated in Figure 1.

Figure 2 shows the photograph of two coupled fibers affected by errors of separation and angular misalinement.

Fig 2 - Coupling between two optical fibers affected by errors of separation s and misalinement α.

These losses can be evaluated by interposing between the two optical fibers a refractive-index adapter, or in free air (in which case losses owing to deviation are also added). The presence of a refractive-index adapter, varying the angles of incidence and emergence, affects the behavior of the loss curve.

APPROVED FOR RELEASE: 2007/02/08: CIA-RDP82-00850R000200040044-7

APPROVED FOR RELEASE: 2007/02/08: CIA-RDP82-00850R000200040044-7

Figures 3 a,b,c show loss curves for linear offset u, separation s, and angular misalinement α relative to Coming C.W. graded-index-profile optical fibers, without a refractive-index adapter. Comparative coupling losses for fibers with core diameters of 60, 80 and 100 m are directly plotted.[8] The test data were obtained using an automated setup, which is diagramed schematically in Figure 4 and photographed in Figure 5.

Similar results have been reported by various authors. For example, see work cited in bibliographical reference 5.

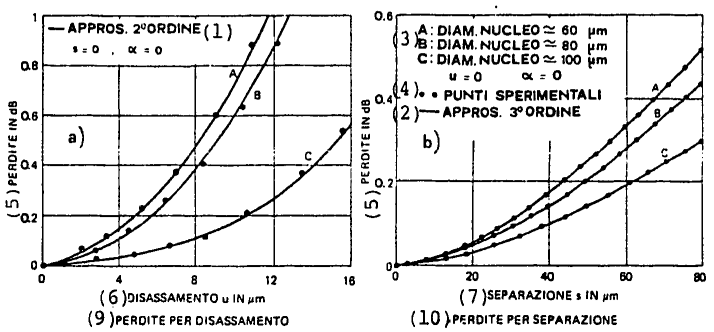

Key:

1. Second order approximation
2. Third order approximation
3. A: Core diameter = 60 μm
   B: Core diameter = 80 μm
   C: Core diameter = 100 μm
4. Experimental points
5. Losses in dB
6. Axial offset u in μm
7. Separation s in μm
8. Angular misalinement α in degrees
9. Axial offset losses
10. Separation losses
11. Angular misalinement losses

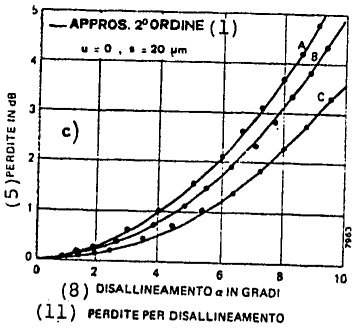

Fig 3 - Coupling losses between two fiber sections owing to: a) axial offset u; b) axial separation s; c) angular misalinement α.

APPROVED FOR RELEASE: 2007/02/08: CIA-RDP82-00850R000200040044-7

APPROVED FOR RELEASE: 2007/02/08: CIA-RDP82-00850R000200040044-7

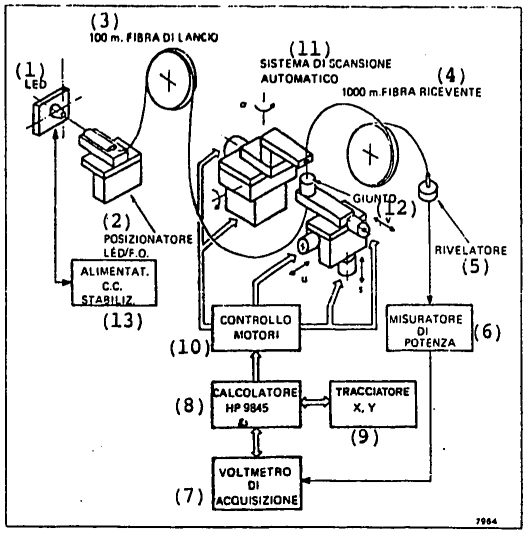

Fig 4 - Schematic block diagram of automated test setup for coupling-loss measurements between optical fibers.

Key:

1. Light emitting diode (LED)
2. LED-optical fiber positioner
3. Launch fiber-100 meters
4. Receiving fiber-1,000 meters
5. Detector
6. Power meter
7. Detection voltmeter
8. HP 9845 Calculator
9. X,Y curve tracer
10. Motor controls
11. Automatic scanning system
12. Joint
13. Stabilized d.c. supply

APPROVED FOR RELEASE: 2007/02/08: CIA-RDP82-00850R000200040044-7

APPROVED FOR RELEASE: 2007/02/08: CIA-RDP82-00850R000200040044-7

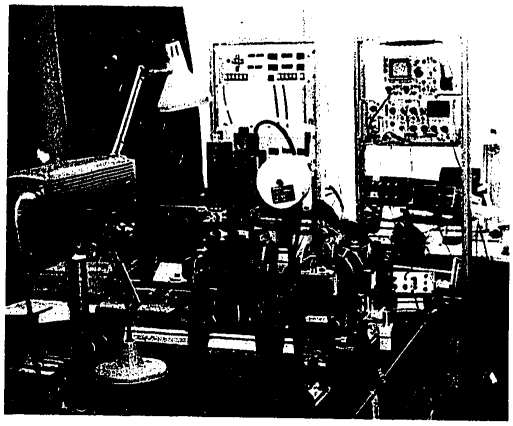

Fig 5 - Automated optical test setup for measurement of coupling errors.

2. Permanent Joints between Single Fibers

To form links many kilometers in length, several optical fiber sections must be jointed. In most cases, these joints must be of the permanent type called "splices," which are not intended to be subjected to repeated connections and disconnections.

Splices may be subdivided into three categories according to the manner in which they are effected:[9]

1) fusion splices,

2) sleeve splices,

3) groove splices.

2.1 Fusion Splices

This technique consists of heating the two ends to be jointed to the point of fusion, for example, by means of an arc discharge, and exerting sufficient pressure axially to obtain a weld between them. This provides continuity of the transmission medium through the point of junction (Figure 6).

APPROVED FOR RELEASE: 2007/02/08: CIA-RDP82-00850R000200040044-7

APPROVED FOR RELEASE: 2007/02/08: CIA-RDP82-00850R000200040044-7

The necessary temperature varies, of course, according to the material of which the fiber is made. Multiple-ingredient-glass fibers require temperatures around 800° C, which are easily obtainable with ordinary, e.g., nickel-chrome, resistances.

Key:

1. Optical Fiber
2. Electrodes
3. Positioners 1 and 2

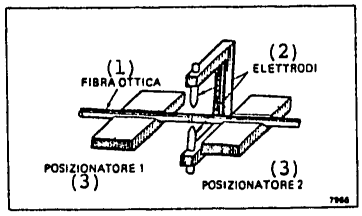

Fig 6 - Diagram of method used to splice optical fibers by the fusion technique.

The most commonly used fibers currently have a high silica content and require much higher temperatures, around 2,000° C, for fusion. Such temperatures are obtainable by means of an electric arc between tungsten electrodes, or by means of a plasma microtorch.

Using this technique, the two fibers can be mutually positioned by observation through a microscope, or by maximizing the transfer of power.

The ends to be spliced are accurately positioned between the two electrodes, in the path of the arc. Typically, the applied voltage ranges between 3,000 and 7,000 volts and discharge current between 10 and 20 milliamperes.

A detailed examination of the problem of cutting and fusion-splicing the fiber is given in bibliographical reference 10, which describes an automatic system for preparing and fusing optical fibers in the field, and analyzes in detail the parameters affecting the characteristics of the joint. The technique used is that of prefusion and fusion, the various phases of which are illustrated in Figure 7. After a preliminary alinement of the two fibers at the proper distance from each other by means of a manual positioning system, the successive phases take place automatically.

A sample statistical distribution of the losses obtained is shown in Figure 8. The average loss measured on $N = 100$ samples of graded-index optical fiber with outside diameter $D_E = 150 \mu m$ and length $l = 100$ m was 0.05 dB.

The principal advantages of joints obtained with the aforementioned techniques derive from the absence of mechanical elements at the point of junction which are cumbersome and sources of fragility; from the perfect

APPROVED FOR RELEASE: 2007/02/08: CIA-RDP82-00850R000200040044-7

APPROVED FOR RELEASE: 2007/02/08: CIA-RDP82-00850R000200040044-7

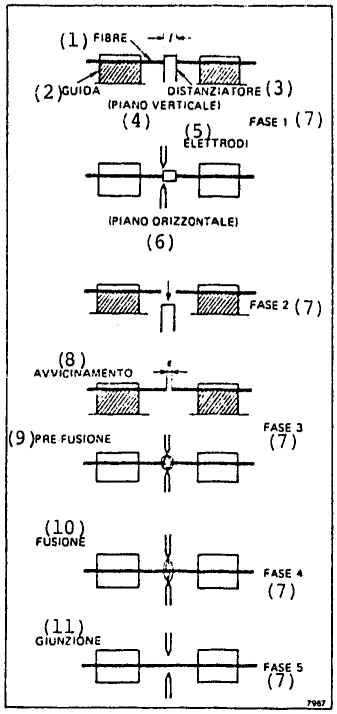

Key:

1. Fiber
2. Guide
3. Spacer
4. Vertical view
5. Electrodes
6. Horizontal view
7. Phases 1 thru 5
8. Approach
9. Prefusion
10. Fusion
11. Splice

Fig 7 - Fusion-splicing procedure.

Key:

1. N = 100 samples
2. Number of samples
3. Losses (dB)

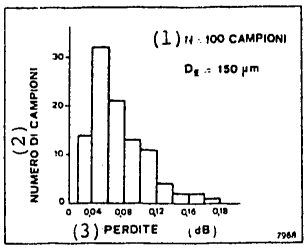

Fig 8 - Statistical distribution of losses in junction of fusion-spliced graded-index optical fibers.

APPROVED FOR RELEASE: 2007/02/08: CIA-RDP82-00850R000200040044-7

APPROVED FOR RELEASE: 2007/02/08: CIA-RDP82-00850R000200040044-7

index-match, which in other types of joints can be only partially achieved through the introduction of properly selected fluids or resins between the two fibers; from the absence of thermal and mechanical stress effects on the transmission characteristics of the joint. Mechanical stress tests showed the maximum tensile strength to be 60 percent of the original, and thermal tests showed no significant changes in characteristics of the joint with changes in temperature.

Among the disadvantages there is the fact that high temperatures can somehow alter the refractive-index profile at the point of fusion, thereby causing a mode conversion; mode conversion phenomena, however, appear to be caused by every type of joint. Lastly, working with high voltages and flames can be a source of danger in field operations, inside small enclosures where explosive gases may be present.

It follows from what has been said, that fusion splicing is one of the more promising techniques, especially with the availability of completely automated equipment for obtaining straightforward, uncluttered joints with field splice losses of the order of 0.1 dB or less.

2.2 Sleeve Splices

This technique is based on the use of sleeves, generally made of glass, whose inside diameter must be as precise as possible, to ensure the correct alinement of the two ends of fiber being spliced. A simplified schematic of the principle involved is given in Figure 9, showing the transverse hole at the midpoint of the sleeve through which a transparent adhesive substance is inserted that provides good mechanical strength and matches the refractive index.

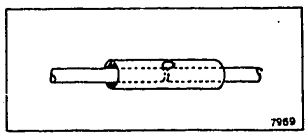

Fig 9 - Structure of sleeve splice

Field application of this technique is described in bibliographical reference 11. The process involved in making this type of splice is diagramed schematically in Figure 10.

The ends of the sleeve are slightly flared to facilitate the insertion of the two fibers. Using this type of splice, losses obtained with step-index optical fibers averaged 0.25 dB ($N = 60$, core diameter $D_N = 85 \mu m$, outside diameter $D_E = 125 \mu m$); with graded-index fibers they averaged 0.21 dB ($N = 20$, $D_N = 85 \mu m$, $D_E = 125 \mu m$).

APPROVED FOR RELEASE: 2007/02/08: CIA-RDP82-00850R000200040044-7

APPROVED FOR RELEASE: 2007/02/08: CIA-RDP82-00850R000200040044-7

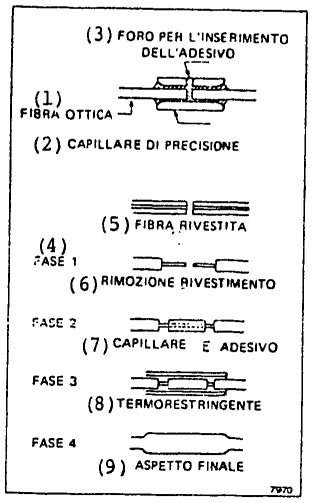

Key:

1. Optical fiber
2. Precision sleeve
3. Hole for insertion of adhesive
4. Stages 1 thru 4
5. Cladded fiber
6. Cladding removed
7. Sleeve and adhesive
8. Heat-shrinkable jacket
9. Finished appearance

Fig 10 - Procedure for making a sleeve splice.

To minimize play of the fibers inside the sleeve, another solution has been proposed,[12] in which one of the fibers is inserted in a pyrex sleeve, whose softening temperature is lower than that of quartz. This assembly is heated to the point where the sleeve, as a result of the stress thus produced, tends to collapse around the fiber (Figure 11); the fiber is then secured inside the sleeve by inserting adhesive. Next, the second fiber is inserted into the other end of the sleeve and the entire assembly secured with epoxy, which has the additional function, previously mentioned, of matching the refractive index. The splice is then enclosed in a protective metal tube. Such a joint presents losses of the order of 0.2-0.3 dB with graded-index fibers ($D_N = 30\,\mu m$, $D_E = 100\,\mu m$, length of each fiber = 100 m).

Key:

1. Sleeve
2. Sleeve collapsed
3. Adhesive

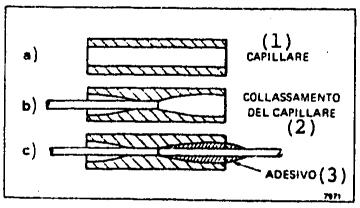

Fig 11 - Stages in making a collapsed-sleeve splice

APPROVED FOR RELEASE: 2007/02/08: CIA-RDP82-00850R000200040044-7

APPROVED FOR RELEASE: 2007/02/08: CIA-RDP82-00850R000200040044-7

Another simple and interesting technique for obtaining a good quality joint[13] is based on the use of a sleeve having a square cross section, which encloses the fibers with considerable play. This method combines two techniques: that of sleeves discussed above for the approximate alinement and protection, and that of grooves (discussed below) for the precise alinement. Neither a microscope nor a micromanipulator is used in this method, illustrated in Figure 12. The two fiber ends are pressed against one of the inside corners of the sleeve while bending the fibers outside the sleeve, and secured there by means of an adhesive that fills the sleeve. For maximum precision, the internal radius of curvature of the corners must be small. It is to be noted that this splice is self-alining, in that externally bending the fibers automatically presses the ends into proper position in the opposite corner.

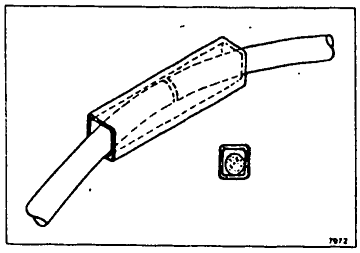

Fig 12 - Square-sleeve splice.

2.3 Groove Splices

Another technique for precision splicing of two optical fibers, including single-mode fibers, uses, in its simplest version, described in bibliographical reference 14, a precisely V-grooved plexiglass base. The two fiber ends to be spliced are inserted in the groove and secured there by a lid.

This type of joint, in which alinement is obtained by means of a V-groove,[15] is illustrated in Figure 13. Alinement is obtained by pressing the fibers into the bottom of the groove. Of the splices tested with step-index optical fibers, 50 percent showed insertion losses of less than 0.2 dB.

APPROVED FOR RELEASE: 2007/02/08: CIA-RDP82-00850R000200040044-7

APPROVED FOR RELEASE: 2007/02/08: CIA-RDP82-00850R000200040044-7

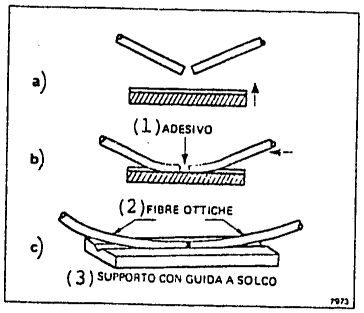

Key:

1. Adhesive
2. Optical fibers
3. Grooved base

Fig 13 - V-groove splice: preparatory stages.

A second splicing method using a groove having good characteristics, called "Springroove"(*),[16] consists of a base and two small cylinders, which together form the groove for the two optical fibers (Figure 14), and an elastic element which keeps the fiber ends positioned while the successive stages of the splice are completed. The cylinders are so dimensioned that the tops of the fibers project above them, facilitating clamping by means of a simple spring device. This method is illustrated in Figure 14 as well as on the cover of this paper. Figure 15 shows the statistical loss distribution on 48 samples, indicating an average value of 0.05 dB with graded profile fibers ($N = 94$, numerical aperture $\Delta = 14$, $D_N = 80\,\mu m$, $D_E = 125\,\mu m$, source: stabilized lamp).

Key:

1: "Springroove" ® (Registered trademark and patented) splice components

2. Sectional view

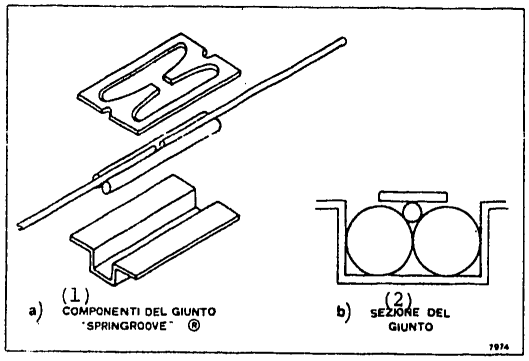

Fig 14 - "Springroove" ® (Registered trademark and patented) splice.

(*) Registered trademark and patented.

APPROVED FOR RELEASE: 2007/02/08: CIA-RDP82-00850R000200040044-7

APPROVED FOR RELEASE: 2007/02/08: CIA-RDP82-00850R000200040044-7

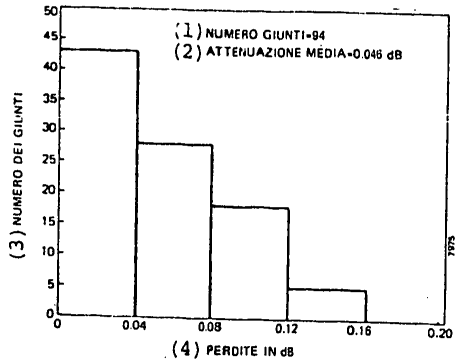

Key:

1. Number of splices = 94
2. Average loss = 0.046 dB
3. Number of splices
4. Losses in dB

Fig 15 - Statical loss distribution of "Springroove" splices.

The principal advantage of this type of splice is that it can be made without optical or mechanical equipment, by simply inserting the fibers manually. The disadvantage, of course, which is common to the other types described in this section as well, is the introduction of a mechanical element of a certain bulk into the splice.

An analogous technique, in which the spring is replaced by a third cylinder[17] pressed against the fiber by a heat-shrinkable jacket, is illustrated in Figure 16. Losses obtained with this method averaged 0.2 dB, using multimode fibers with $D_N = 80 \mu m$.

Key:

1. Heat-shrinkable jacket
2. Cylindrical guides for axial alinement
3. Optical fibers

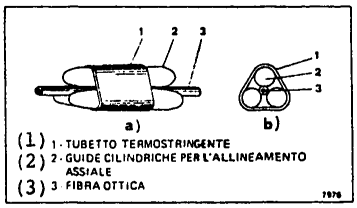

Fig 16 - 3-cylinder splice.

3. Permanent Splices for Multiple-Fiber Cables

The groove technique proves useful from the viewpoint of a base with multiple grooves for splicing the multiple fibers of a laminated flat ribbon-cable.

APPROVED FOR RELEASE: 2007/02/08: CIA-RDP82-00850R000200040044-7

APPROVED FOR RELEASE: 2007/02/08: CIA-RDP82-00850R000200040044-7

A splice of this type[18] was made using parallel grooves engraved in a plastic base by means of a suitably designed instrument. The two properly prepared cable-ends are slid into prealinement slots, then pressed into the grooves. Reciprocal fiber-ends thus automatically meet each other in proper alinement without requiring the use of a microscope. A cover is cemented over the top to ensure mechanical stability. Glycerine is used to match the refractive index. Measured losses average 0.12 dB ($N = 120$, $D_N = 92$, $D_E = 130$, $L_1 = 1$ m, $L_2 = 1$ m, source: 6,328 Å laser). A splice of this type is illustrated in Figure 17.

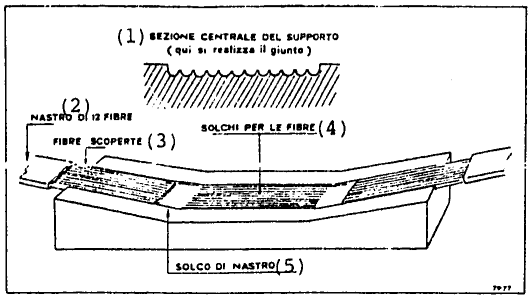

Key:

1. Section across center of base (junction takes place here)
2. 12-fiber ribbon cable
3. Uncladded fibers
4. Grooves for fibers
5. Cable slot

Fig 17 - Multiple splice for ribbon cable, based on groove principle.

A similar splice for multi-ribbon cables but containing 12 groups of 12 grooves each (Figure 18), all adjacent to each other in the same plane, is discussed in bibliographical reference 19. This splice is made by die-casting, using a metallic die to bind the bases in polycarbonate with optimum precision and reproducibility.

Key:

1. 12-fiber ribbon
2. Ribbon grooves
3. Splice
4. Fiber grooves
5. 1st ribbon
6. 12th ribbon

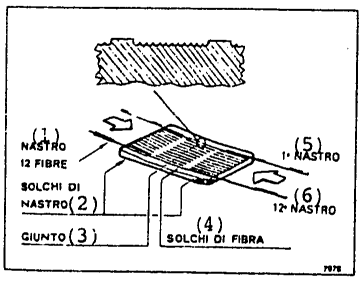

Fig 18 - Multiple splice for multi-ribbon cable.

APPROVED FOR RELEASE: 2007/02/08: CIA-RDP82-00850R000200040044-7

APPROVED FOR RELEASE: 2007/02/08: CIA-RDP82-00850R000200040044-7

The advantages of the two above-mentioned techniques are brought together in still another type of multiple splice.[20] The casing and lid of the splice are cast in polycarbonate by a die and injection molding technique suited to volume production. They enclose a silica-glass base having precision grooves, preferably made by an etching process.

After proper preparation, the two ends of the fibers are inserted in the grooves and brought together. The fibers are secured by means of a lid having a center hole for the injection of an adhesive which also matches the refractive index.

The two ends of the joint are then placed in a mold into which a resin is poured to provide the needed reinforcement. With graded-index fibers, average losses are 0.22 dB ($N = 111$, $D_N = 55\,\mu m$, $D_E = 110\,\mu m$).

Using a type of cable such as proposed in bibliographical reference 21, which, instead of being constructed in overlying layers, has a circular cross-section, with the fibers lying in machined grooves along the outer surface of a cylindrical core (Figure 19), another splicing technique has given good results.

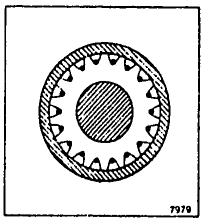

Fig 19 - Cross-section of cable with star-shaped core.

After cutting back the cable sheath to expose the fiber-ends to be jointed, a short section of the star-shaped core is removed and replaced with a like section having precise, perfectly matching grooves. The exposed fibers are pressed into these grooves and cemented in place, after which a single cut is made across the fiber-ends and through the new supporting section, and a suitable refractive-index matching coating applied. After preparing both cable-ends in this manner, they are brought together and secured by semicylindrical casings and alinement cylinders.

Greater precision can be obtained by machining the two grooved support sections from a single piece of alumina. Losses obtained in this manner with step-index fibers averaged 0.3 dB ($N = 40$, $D_N = 65\,\mu m$, $D_E = 110\,\mu m$, $l_1 = 500$ m, $l_2 = 30$ m, source: laser diode).

APPROVED FOR RELEASE: 2007/02/08: CIA-RDP82-00850R000200040044-7

APPROVED FOR RELEASE: 2007/02/08: CIA-RDP82-00850R000200040044-7

4. Connectors for Single Fibers

The purpose of this section is to discuss some of the more common types of connectors designed to permit repeated connection and disconnection of optical fibers and cables:

Generally speaking, these types may be classified according to their basic operating principles. They are:

1) Cylinder-and-watch-jewel connectors

2) Groove connectors, with grooves formed in various manners

3) Concentric cylinder connectors

4) Eccentric cylinder connectors

5) Molded connectors

6) Beam expansion connectors

7) Other types

In general, the principal characteristics on which a connector is evaluated are: small insertion losses, ease of fabrication and assembly, small variations in losses even after a large number of connections and disconnections, wide interchangeability of connectors, insensitivity to environmental factors (temperature and dust), low cost, low crosstalk in multiple connectors.

We proceed now to a detailed discussion of the above connector types.

4.1 Cylinder-and-watch-jewel Connectors

This type of connector, of simple design, consists of a watch jewel mounted in the tip of a metallic cylinder. Its precision depends upon that of the hole in the jewel, the purpose of which is to center the fiber with respect to the cylinder. The latter acts as the guide for the optical fiber, which is secured to it with adhesive. The two cylinder-equipped fiber-ends are then inserted into a metallic sleeve which alines them.

Both the cylinder and the external sleeve are commercially available shelf-items with tolerances representing an average loss of 1 dB (with step-index optical fibers having core diameters of 75-100 μm). A connector of this type, described in bibliographical reference 22, is diagramed in Figure 20.

APPROVED FOR RELEASE: 2007/02/08: CIA-RDP82-00850R000200040044-7

APPROVED FOR RELEASE: 2007/02/08: CIA-RDP82-00850R000200040044-7

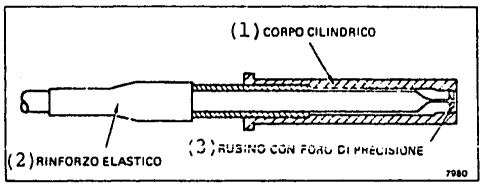

Key:

1. Cylindrical casing
2. Resilient reinforcement
3. Watch-jewel with precision hole

Fig 20 - Cylinder-and-watch-jewel connector with precision hole

4.2 Groove Connectors

In a more complex type of connector[23] the fiber is positioned in a groove formed by two spheres and held in place by a third sphere (Figure 21a). The three spheres holding the fiber are then inserted in a specially designed sleeve. Pressing the two groups of three spheres against each other, they rotate into a reciprocally seated position, representing a relative rotation of 60 degrees. The two fibers are thus automatically alined (Figure 21b). So that the two fibers will not strike each other, each must be backed away from the plane tangent to its three spheres. The fibers are secured in the centering system with adhesive.

Key:

1. Fiber
2. Junction plane

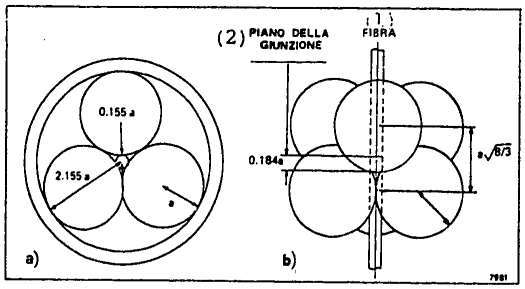

Fig 21 - Triple-ball connector: a) cross-section;
b) diagram of optical fiber positioning system.

The longitudinal positioning of the fibers requires the use of a microscope. The sole precision parts are the tungsten carbide spheres, which are available within the necessary precision limits.

This connector shows a loss of 0.5 dB using step-index optical fiber (numerical aperture $\Delta = 0.56$, $D_E = 125\,\mu m$, $D_N = 80\,\mu m$).

APPROVED FOR RELEASE: 2007/02/08: CIA-RDP82-00850R000200040044-7

APPROVED FOR RELEASE: 2007/02/08: CIA-RDP82-00850R000200040044-7

4.3 Concentric Cylinder Connectors

A concentric cylinder connector is described in bibliographical reference 24. The aim of its designers is to achieve a connector with losses less than 0.7 dB, of which 0.3 dB represent reflection losses and 0.4 dB those owing to imperfections in the connector. Of the latter, 0.3 dB are attributed to offset u and 0.10 dB to separation s. With step-index fibers having $D_N = 60\,\mu m$, $D_E = 150\,\mu m$ and $\Delta = 0.17$, the mechanical constraints are: $u \leq 5\,\mu m$ and $\alpha \leq 1^\circ$.

The connector consists of two male plugs that are inserted in a central adapter which serves as a guide and locking sleeve (Figure 22). The fiber is secured with adhesive inside a glass sleeve that is in turn secured inside a stainless steel tube. Having thus assembled the fibers, their ends are prepared and the pivot centered and secured with adhesive inside a cylinder. The latter is accomplished by using a second alinement-cylinder, a microscope and a television camera to monitor the centering; the adhesive is then injected between the pivot and the cylinder. Finally, the connection is made by means of an adapter that joins and alines the two cylinders. Losses with this connector, without refractive-index adapter, average 0.49 dB with step-index optical fibers ($\Delta = 0.17$, $D_N = 60\,\mu m$, $D_E = 150\,\mu m$, $N = 140$).

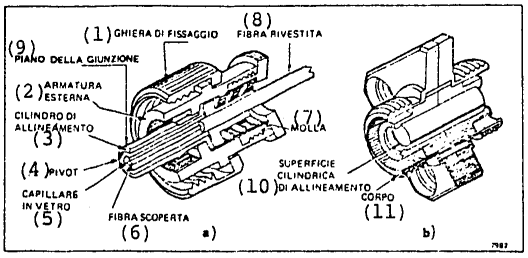

Key:

1. Locking sleeve
2. Outside reinforcement
3. Alinement cylinder
4. Pivot
5. Glass sleeve
6. Uncladded fiber
7. Spring
8. Cladded fiber
9. Plane of joint
10. Cylindrical alinement surface
11. Casing

Fig 22 - Sectional detail of concentric cylinder connector for optical fibers.

APPROVED FOR RELEASE: 2007/02/08: CIA-RDP82-00850R000200040044-7

APPROVED FOR RELEASE: 2007/02/08: CIA-RDP82-00850R000200040044-7

Similar to the preceding one in principle and compatible with it operationally is the connector described in bibliographical reference 25, differing from it, however, in two respects. The central adapter in the latter consists of a mandrel-type sleeve that can clamp and aline two cylinders even of slightly different diameters (Figure 23a,b,c(.

Key:

1. Body
2. Clamping sleeve
3. Outside armature of mandrel
4. Alinement cylinders

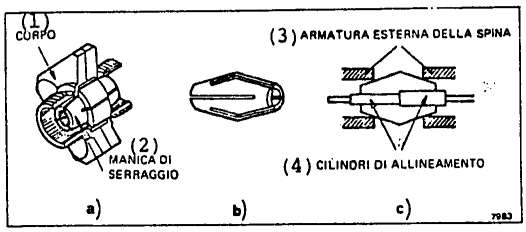

Fig 23 - Concentric cylinder connector for optical fibers: a) center adapter, b) clamping sleeve, c) operating principle.

Moreover, the connector is not assembled by centering the core in the cylinder, then securing it with adhesive. The technique developed by its authors consists of securing the cylinder that contains the fiber (previously prepared) inside the external cylinder with adhesive. The external cylinder is then placed in the headstock of a lathe and observed through a microscope in the position of the tailstock. The mandrel that clamps the cylinder can thus be positioned so that the center of the core exactly coincides with the rotating axis of the lathe. The outside surface of the cylinder is then turned down with the lathe tool to perfect concentricity with the fiber core, within the precision limits of the lathe.

The designers have sought to build a connector with losses of less than 0.3 dB, exclusive of reflection losses. This involves working to tolerances of 6 μm of lateral offset, 1° of angular misalinement, and 10 μm of axial separation ($D_N = 65\ \mu m$). Average losses obtained, without refractive-index adapter, were 0.4 dB with graded-index fibers ($N = 40$).

4.4 Eccentric Cylinder Connectors

We discuss now a connector that uses the principle of the double eccentric[2] for the preliminary centering and alinement, through a microscope, of the optical fiber it encloses. Its basic structure, as can be seen in Figure 24, consists of three eccentric tubes, one external (1), one intermediate (2), and one internal (3) tube in which the optical fiber is eccentrically secured.

APPROVED FOR RELEASE: 2007/02/08: CIA-RDP82-00850R000200040044-7

APPROVED FOR RELEASE: 2007/02/08: CIA-RDP82-00850R000200040044-7

Key:

1. External eccentric
2. Intermediate eccentric
3. Internal eccentric
4. Optical fiber core
5. Area within which core center can be moved

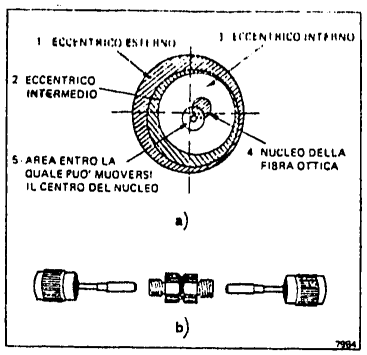

Fig 24 - a) Structure of triple-eccentric connector; b) view of entire connector.

If the inside and outside diameters of tube 3 containing the fiber are suitable chosen, it will always be possible, by rotation, to bring the center of the outside circumference of tube 1 into coincidence with the center of the core of the optical fiber.

This is done with the aid of a microscope and a reference-cylinder.

When the two cylinders have thus been centered and secured mechanically, they are inserted into a central adapter to complete the connector.

Average losses without refractive-index adapter are 0.57 dB using graded-index fibers ($N = 20$, laser source: 6,328 Å).

Still based on the eccentric principle, another connector uses an innovative system of alinement.[26] It consists of an eccentric assembly of the fibers inside of two axially offset cylinders, held in a groove by a coil spring. The groove is made up of two transversely offset sections, as shown in Figure 25a. The fiber is enclosed in a sleeve (Figure 25b) whose end opposite the end to be connected is cut at a 45-degree angle, so that the light that is not coupled because of misalinement is totally reflected and is gathered perpendicularly to the axis of the fiber by a detector that is contained within the connector itself. To obtain optimum coupling, the two halves of the coupling are simply rotated with respect to each other until minimum output is obtained from the detector.

Average losses obtained with refractive-index adapter were 0.087 dB for step-index optical fibers ($\Delta = 0.48$, $D_N = 85\,\mu m$, $D_E = 105\,\mu m$); for graded-index fibers, losses averaged 0.098 dB ($\Delta = 0.18$, $D_N = 63\,\mu m$, $D_E = 130\,\mu m$).

APPROVED FOR RELEASE: 2007/02/08: CIA-RDP82-00850R000200040044-7

APPROVED FOR RELEASE: 2007/02/08: CIA-RDP82-00850R000200040044-7

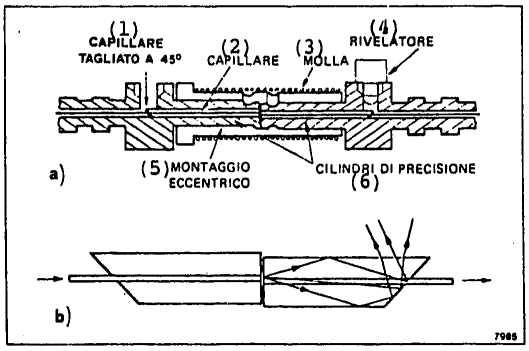

Key:

1. Sleeve cut at 45 degrees
2. Sleeve
3. Spring
4. Detector
5. Eccentric mounting
6. Precision cylinders

Fig 25 - a) Sectional view of eccentric-cylinder connector with loss detector; b) misalinement loss detection system detail.

4.5 Molded Connectors

These are made by direct-molding two male plastic cones around the two fibers, which are then alined by a central adapter.[27] Its authors have sought with this system to design a connector having a lateral offset error of less than 3 μm and a separation error of less than 40 μm, using fibers with $D_N = 55\ \mu m$ and $D_E = 110\ \mu m$.

The material used to heat-mold the male cones, epoxy with a quartz-dust aggregate, does not damage the fiber during this recladding. Moreover, the material, labor and assembly involved are not costly.

The precision element required for alinement is provided by the conical surfaces, which are obtained by means of dies made with a precision better than 1 μm.

Key:

1. Male cone
2. Uncladded fibers
3. Central alinement adapter
4. Protective bushings
5. Cladded fiber

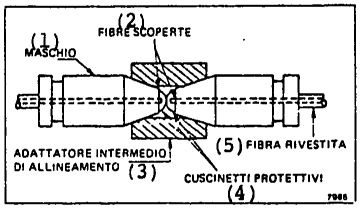

Fig 26 - Molded connector. Cross-section of the two male cones and central adapter.

APPROVED FOR RELEASE: 2007/02/08: CIA-RDP82-00850R000200040044-7

APPROVED FOR RELEASE: 2007/02/08: CIA-RDP82-00850R000200040044-7

The biconical central adapter (Figure 26) is also molded on a precision mandrel, assuring a concentricity of better than 1μm between the two cones. This is all accomplished by a routine process. Losses in 50 samples averaged 0.3 dB. Connect-disconnect tests were also carried out. In 100 operations, 90 percent of the cases resulted in losses coinciding with initial losses within 0.02 dB. Temperature variations between 0 and 60 degrees C produced no measurable loss variations.

4.6 Beam Expansion Connectors

Another technique consists of collimating the normally divergent beam from one of the fibers, and, through a second optic, focusing it on the core of the receiving fiber. The purpose of this technique is to be able to work with less constrictive lateral and longitudinal tolerances than those we have considered up to this point (at the trade-off cost of a more critical angular alinement which, however, is more easily achieved).

Connectors of this type are designed using various optical principles: tapers, lenses, couplers and grating, and spheres.

The design principle of one of these,[28] using two sapphire spheres having a refractive index n = 1.77 and a radius of 1.5μm, is indicated in Figure 27.

Key:

1. Reference plane
2. Spherical lenses
3. Fiber

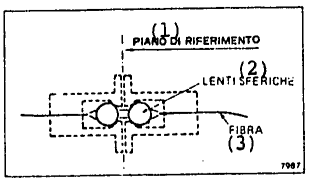

Fig 27 - Schematic diagram of connector using spherical lenses.

The two lenses form a 1:1 image of the end of the transmitting fiber on the end of the receiving one. So that the centering of the image will be independent of relative rotation of the two ends at the instant of securing them, the optical axes of the two fibers must be perpendicular to a reference plane indicated in Figure 27. Using fibers with a parabolic profile, average losses of 1 dB ($N = 20$, $D_N = 50\mu m$, $\Delta = 0.2$) were obtained. (Subsequent rotation can increase losses by 5 percent.) These losses could be reduced by using spheres coated with a nonreflective material.

APPROVED FOR RELEASE: 2007/02/08: CIA-RDP82-00850R000200040044-7

APPROVED FOR RELEASE: 2007/02/08: CIA-RDP82-00850R000200040044-7

5. Connectors for Multiple-fiber Cables

The operating principle of groove connectors for the coupling of optical fibers is discussed in subsection 4.2. This principle is also applied with good results in the construction of multiple connectors.

The design techniques vary, but they are reducible to two basic types: grooves obtained by mechanical processes, and grooves obtained by etching processes.

A multiple connector has been designed that obtains the desired grooves by means of parallel and contiguous cylinders and permits the alinement and connection of several fibers simultaneously.[1,29]

The groove system consists either of two arrays of discrete cylinders (Figure 28a), or of contiguous semicylinders machined directly from a single piece (Figure 28b). The cylinders used are made either of plastic or of metal coated with a plastic whose inherent elasticity permits the locking in and alinement of the fibers by suitable pressure. The practical version of this connector is equipped with a system for regulating the separation between the ends, based on a section of slack in which the fiber can curve freely as shown in Figure 29. The connector also incorporates a suitable resilient cable-clamping system.

Key:

1. Cement
2. Optical fibers

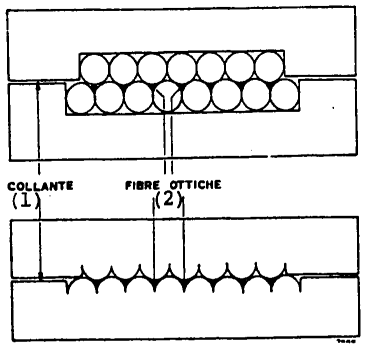

Fig 28 - Alinement array schemes: a) discrete cylinder method; b) monolithic method.

APPROVED FOR RELEASE: 2007/02/08: CIA-RDP82-00850R000200040044-7

APPROVED FOR RELEASE: 2007/02/08: CIA-RDP82-00850R000200040044-7

Key:

1. Cable
2. Cable clamped
3. Fibers tightly clamped
4. Slack zone
5. Fibers lightly clamped
6. Coupling zone
7. Overlap zone
8. Flat metallic base
9. Optical fibers
10. Cable

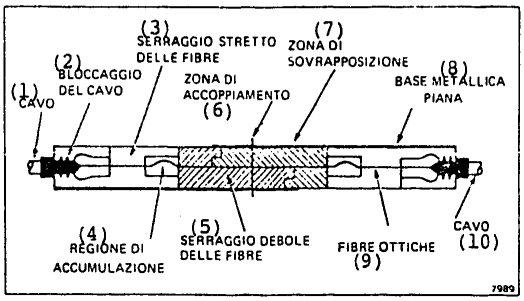

Fig 29 - Stacked discrete-cylinder multiple connector: longitudinal cross-section.

Its characteristics, measured with step-index fibers ($\Delta = 0.18$, $D_N = 85\,\mu m$, $D_E = 125\,\mu m$, $N = 44$), show an average loss of 0.57 dB (with refractive-index adapter).

Another connector based also on the groove principle permits the connection of several fibers. It consists of a single cylinder with parallel machined V-grooves along the long axis of its surface; these grooves provide seats for the fibers. To ensure a perfect fit between the two halves to be coupled, they are machined as a single grooved cylinder, then cut in two.[30]

The design objective is to obtain insertion losses of not more than 0.1 dB. Assuming lateral offset to be the only source of error, for step-index fibers this signifies a tolerance constraint of less than 2 percent in the core diameter D_N. The properly prepared fiber-ends are secured in the grooves with adhesive, their tips flush with the edge of the cylinder. The cylinder has one groove that is deeper than the others, designed to accommodate a metallic pin that serves to aline the two halves when they are pressed against two other metallic base-pins, as shown in Figure 30.

Losses of less than 0.1 dB have been experienced with step-index optical fibers ($\Delta = 0.56$, $D_N = 60\,\mu m$).

It was noted, furthermore, that insertion losses were not affected by temperature variations in the range below 100 degrees C.

This connector, given its low losses, should be suitable for coupling single-mode optical fibers.

APPROVED FOR RELEASE: 2007/02/08: CIA-RDP82-00850R000200040044-7

APPROVED FOR RELEASE: 2007/02/08: CIA-RDP82-00850R000200040044-7

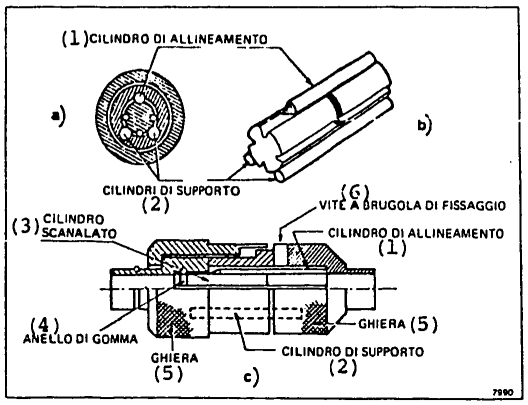

Key:

1. Alinement pin
2. Base pins
3. Grooved cylinder
4. Rubber ring
5. Array
6. "Brugola-type" securing screw

Fig 30 - Grooved cylindrical core multiple connector: a) alinement mechanism; b) sectional view of connector.

The connector described in bibliographical reference 31, based on the groove principle, is suitable for coupling all the fibers of two multi-ribbon cables, by bringing together the two halves of the connector that have previously been fixed to the cable-ends. Obviously, the two halves must ensure the orderly coupling of corresponding optical fibers. All the fibers of one cable-end are arranged in a uniform matrix, the geometry of which is secured by an adhesive, and the fiber ends of that cable are then prepared all at the same time. The other cable likewise having been prepared, the two connector halves are joined. The preliminary alinement is obtained by means of precision grooves machined in the surface of metallic plates (Figure 31), or etched by photolithographic techniques in silicon chips cut according to the (100) axis.

Key:

1. Plane of joint
2. Grooved securing plate
3. Multi-ribbon cable
4. Fibers

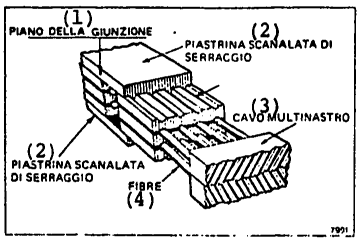

Fig 31 - Stacked-array connector for multi-ribbon optical fiber cables.

APPROVED FOR RELEASE: 2007/02/08: CIA-RDP82-00850R000200040044-7

APPROVED FOR RELEASE: 2007/02/08: CIA-RDP82-00850R000200040044-7

In both cases, the fibers are arranged in layers between the chips, and the interstices are filled with adhesive (Figure 32). The top and bottom sections of the chip stacks thus formed do not contain fibers, so that their grooves can serve as guides for the connection of the two halves.

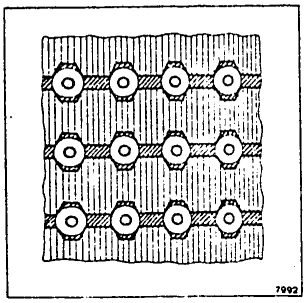

Fig 32 - Partial end view of a multiple, multi-ribbon connector, showing fibers seated in grooves obtained by etching.

The etching of grooves on silicon chips appears to result in more accurately produced guides, in that periodic error, width, vertical alinement and variations in chip thickness can all be kept within a tolerance of 1 μm, while angular misalinement of the grooves is found to be virtually nonexistent.

Connectors of this type yield losses of 0.2-0.3 dB, using a refractive-index adapter, with 12 x 12 multi-ribbon cables using graded-index fibers ($D_N = 55\,\mu m$, $D_E = 110\,\mu m$).

Lastly, bibliographical reference 32 describes an etching technique by which rectangular grooves of suitable width and depth for proper positioning of the fibers to be connected can be produced in thick chips made of a photosensitive plastic material (Figure 33).

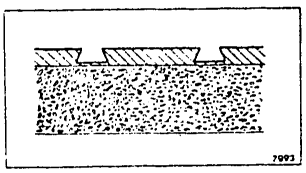

Fig 33 - Multiple-connector alinement grooves obtained by etching in plastic.

APPROVED FOR RELEASE: 2007/02/08: CIA-RDP82-00850R000200040044-7

APPROVED FOR RELEASE: 2007/02/08: CIA-RDP82-00850R000200040044-7

With proper time exposure the grooves can be made slightly ($\simeq$10 m) smaller than the diameters of the fibers, so that the latter can be secured elastically in the grooves by a suitably designed cover.

Alinement of the fibers is obtained by applying two orthogonal forces (Figure 34) that press the fiber-ends to be connected against angled guides.

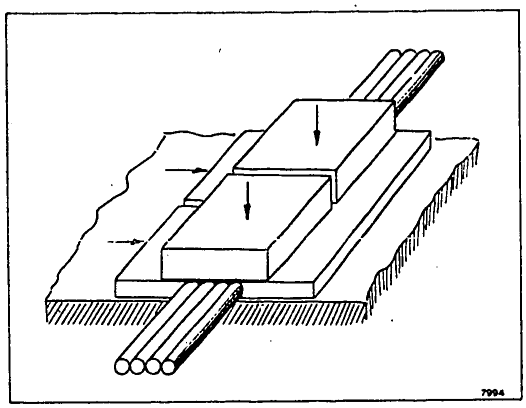

Fig 34 - Assembly diagram of etched-plastic multiple connector; arrows indicate directions in which the connector's movable chips are pressed against the base chip to secure the fibers.

From insertion loss statistics, an average axial offset of 3μm has been estimated.

The characteristics of this connector indicate an insertion loss of 0.2 dB with refractive-index adapter and step-index fibers ($\Delta = 0.14$, $D_N = 92\mu m$, $D_E = 132\mu m$, source: 6,328 Å laser).

6. Conclusions

This paper has examined the basic parameters that define the optical power losses in the coupling of two optical fibers, then described in detail the various techniques involved in designs of permanent and temporary joints, citing for each type described its performance characteristics.

It appears from the foregoing that the jointing problem, which has always been considered a key point in the practical application of fiber optics to telecommunications, has been satisfactorily resolved in several ways.

APPROVED FOR RELEASE: 2007/02/08: CIA-RDP82-00850R000200040044-7

APPROVED FOR RELEASE: 2007/02/08: CIA-RDP82-00850R000200040044-7

Some further considerations, however, are in order. Very low loss joints have been obtained between fiber sections having almost identical geometrical and optical characteristics. In practice, when fiber sections must be jointed, normal variations in their characteristics (outside diameter, core diameter, core-cladding concentricity, numerical aperture), deriving from the production process, can lead to relatively high losses, greater than 1 dB, even with expertly executed joints. This situation can be especially serious where very low loss fibers (1 dB/km) are to be coupled for operation at wavelengths in the region of 1.3μm. Obviously, in this case, the insertion loss of the joint can be the equivalent of adding 1 km of fiber. In view of this requirement, however, a major project is being carried out by international (CCITT) organizations set up specifically for this purpose, to arrive at a standardization of optical fiber characteristics for telecommunications, and to establish the most constrictive feasible tolerances on acceptable variations in these characteristics.

Acknowledgements

We thank Dr B. Costa for the helpful advice he has provided during the writing and revisions of this paper.

BIBLIOGRAPHY

1. Thiel, F.L. and others: "Optical Waveguide Cable Connection" in APPLIED OPTICS, 15, no 11 (November 1976), pp 2785-2791.

2. Tsuchiya, H. and others: "Double Eccentric Connectors for Optical Fibers" in APPLIED OPTICS, 16, no 5 (May 1977), pp 1323-1331.

3. Miller, C.M.: "Transmission vs. Transverse Offset for Parabolic-Profile Fiber Splices with Unequal Core Diameters" in B.S.T.J., 55, no 7, (Sept 1976), pp 917-928.

4. Di Vita, P.; Rossi, U.: "Theory of Power Coupling Between Multimode Optical Fibres" in OPTICAL AND QUANTUM ELECTRONICS, 10, 1978, pp 107-117.

5. Gloge, D.: "Offset and Tilt Loss in Optical Fiber Splices" in B.S.T.J., 55, no 7 (Sept 1976), pp 905-916.

6. Miller, C.M. and others: "A Loss Model for Parabolic-Profile Fiber Splices" in B.S.T.J., 57, no 9 (Nov 1978), pp 3167-3180.

7. Di Vita, P.; Rossi, U.: "A Method for the Evaluation of Tolerances in the Design of Joints Between Multimode Optical Fibres" in CSELT [Telecommunications Research and Study Center (Italy)] RAPPORTO TECNICO, V, no 3, Jun 1977, pp 179-181.

APPROVED FOR RELEASE: 2007/02/08: CIA-RDP82-00850R000200040044-7

APPROVED FOR RELEASE: 2007/02/08: CIA-RDP82-00850R000200040044-7

8. Cocito, G. and others: "Coupling Loss for Three Different Fibre Core Diameters" in CSELT RAPPORTO TECNICO, VI, no 2, Jun 1978, pp 113-119.

9. Miller, C.M.: "Optical Fiber Splicing" in "Topical Meeting on Optical Fibre Transmission," Feb 22-24, 1977, Williamsburg, Virginia, pp WA3, 1-2.

10. Sakamoto, K. and others: "The Automatic Splicing Machine Employing Electric Arc Fusion" in "Fourth European Conference on Optical Communication," Genoa, Sept 12-15, 1978, pp 296-303.

11. Murata, H. and others: "Connection of Optical Fiber Cable" in "Topical Meeting on Optical Fiber Transmission," Jan 7-9, 1975, Williamsburg, Virginia, pp WA5, 1-4.

12. Dalgoutte, D.G.: "Collapsed Sleeve Splices for Field Jointing of Optical Fibre Cable" in "Third European Conference on Optical Communication," Munich, Sept 14-16, 1977, pp 106-108.

13. Miller, C.M.: "Loose Tube Splices for Optical Fibers" in "First European Conference on Optical Fibre Communication," London, Sept 16-18, 1975, pp 90-82 [as published].

14. Someda, C.G.: "Simple, Low Loss Joints Between Single Mode Optical Fibers" in B.S,T.J., 52, no 4, (Apr 1973), pp 583-597.

15. Kunze, D. and others: "Jointing Techniques for Optical Cables" in "Second European Conference on Optical Communication," Paris, Sept 27-30, pp 257-260.

16. Cocito, G. and others: "First Report on COS 2 Experimental Results" in NTZ, 31, 2, 1978, pp 135-137.

17. Tsuchiya, H. and others: "Loss of Double Eccentric Connectors for Optical Fibres" in "Paper of the Technical Group on Optics and Quantum Electronics, IECE," Japan, 1975.

18. Cherin, A.H.; Rich P.J.: "Multigroove Embossed-plastic Splice Connector for Joining Groups of Optical Fibers" in APPLIED OPTICS, 14, 12, Dec 1975, pp 3026-3030.

19. Cherin, A.H.; Rich, P.J.: "An Injection-Molded Plastic Connector for Splicing Optical Cables" in B.S.T.J., 65, no 8 (Mar 1975), pp 1057-1067.

20. Cherin, A.H.; Rich, P.J.: "An Injection Molded Splice Connector with Silicon Chip Insert for Joining Optical Fiber Ribbons" in "Topical Meeting on Optical Fibre Transmission," Feb 22-24, 1977, Williamsburg, Virginia, pp WA7, 1-4.

APPROVED FOR RELEASE: 2007/02/08: CIA-RDP82-00850R000200040044-7

APPROVED FOR RELEASE: 2007/02/08: CIA-RDP82-00850R000200040044-7

21. Le Noane, G.; De Vecchis, M.: "Further Developments on Compartmented Fiber Optic Cable Structure and Associated Splicing Technique" in IOOC '77, B 10-5.

22. Archer, J.D.; Tech, B: "Fibre Optics Interconnection Components" in AGARD-CPP-219, 1977, pp 52-1, 52-8.

23. Hensel, P.: "Triple Ball Connector for Optical Fibre" ELECTRONICS LETTERS, 13, 24,, 24th Nov 1977, pp 734-735.

24. Suzuki, N. and others: "A New Demountable Connector Developed for a Trial Optical Transmission System" in IOOC, Jul 18-20, 1977, pp 351-354.

25. Kurochi, N. and others: "A Development Study on Design and Fabrication of an Optical Fiber Connector" in "Third European Conference on Optical Communication," Sept 14, 16, 1977, pp 97-99.

26. Vucins, V.: "Adjustable Single-fiber Connector with Monitor Output" in "Third European Conference on Optical Communication," Sept 14, 16, 1977, pp 100-102.

27. Runge, P.K. and others: "Precision Transfer Molded Single Fiber Optic Connector and Encapsulated Connectorized Devices" in "Topical Meeting on Optical Fibre Transmission," Feb 22-24, 1977, Williamsburg, Virginia, pp WA4, 1-4.

28. Nicia, A.: "Practical Low Loss Connector Lens Connector for Optical Fibre" in ELECTRONICS LETTERS, 3rd Aug 1978, vol 4 no 16, pp 511-512.

29. Nicia, A.: "Fiber Optic Cable Getting Connector for Use in Field" in ELECTRONICS, Aug 21, 1975, pp 29-30.

30. Guttman, J. and others: "Multi-pole Optical Fibre-Fibre Connector" in "First European Conference on Optical Fibre Communication," London, 16-18 Sept 1975, pp 96 98 [as published].

31. Miller, C.M.: "Fiber Optic Array Splicing with Etched Silicon Chips" in B.S.T.J., 57, 1 (Jan 1978), pp 75-90.

32. Auracher, F.; Zeitler, K.K.: "Multiple Fiber Connectors for Multimode Fibers" in OPTICS COMMUNICATIONS, 18, no 4, 1976, pp 556-558.

COPYRIGHT: 1974 BY ERI-EDIZIONI RAI TADIOTELEVISIONE ITALIANA

9399

CSO: 5500

APPROVED FOR RELEASE: 2007/02/08: CIA-RDP82-00850R000200040044-7

APPROVED FOR RELEASE: 2007/02/08: CIA-RDP82-00850R000200040044-7

USSR

UDC 621.317.799:621.395.44

MONITORING TRANSMISSION BREAKS ON MAIN COAXIAL CABLES

Moscow ELEKTROSVYAZ' in Russian No 10, 1979 pp 9-11

/Article by N. E. Popova, A. A. Rozhdestvenskiy, A. I. Fukson/

/Text/ Studies are presently being conducted of transmission breaks which adversely affect the quality of communications on canals and channels of communications networks. Ten series of studies of breaks have already been carried out under the auspices of MKKTT/International Telegraph and Telephone Consultative Committee/.

Special equipment has been developed to accumulate data over a long period of time on the number of breaks, their causes, the distribution of breaks by time and length, etc. with the aim of effectively monitoring breaks. The equipment can also be used for the continuous monitoring of canals and channels, the speeding up of the localization process, the detection of short-term breaks, and the prevention of lengthy failures.

Monitoring equipment mock-ups were manufactured in 1976-77. The equipment was tested on a line equipped with a K-1920 device. With slight modification it can be used to study and monitor group and line channels on K-300, K-1920P, K-3600, and other systems.

The Purpose of Monitoring--Studies conducted over many years in our country and abroad show that short-term communications breaks cause 70-80 percent of errors in the transmission of digital information over communications channels,[1] and significantly influence the signal transmission quality of other types of data.[2] The causes of short-term breaks have been largely determined and a typical distribution of them has been presented, for example, in bibliographic entry 2 where breaks resulting from damage make up 55 percent, and those due to maintenance and construction work amount to 29 and 16 percent respectively. This distribution changes for the different lines and network channels depending on the transmission system used, the qualifications of the technical personnel, etc.

Work on decreasing the number of breaks always includes the following stages: 1) determining the chief causes and sources of breaks for a given line or channel by accumulating data over a sufficiently lengthy period of time; 2) immediately notifying technical personnel of the appearance of breaks, and the localization of the sources of breaks; 3) developing and implementing measures to eliminate the causes of breaks.

APPROVED FOR RELEASE: 2007/02/08: CIA-RDP82-00850R000200040044-7

APPROVED FOR RELEASE: 2007/02/08: CIA-RDP82-00850R000200040044-7

The break-monitoring equipment permits an effective solution to the first two problems and is already being used in a number of countries.[2,3]

The Method and Block Diagram of Monitoring--Prolonged observation of the level of the KCh/pilot frequency/ signal is the most convenient and effective way of obtaining accurate information on transmission breaks.[3] Such a monitoring method ensures that breaks will be held to several milliseconds in duration; that the monitored channel will not be loaded with additional test signals; that the accuracy of fixing the amplitude of breaks will be increased so long as the KCh has the greatest lasting stability of the level in the frequency range of the channel.; and that full standardization of the monitoring equipment of the line's intermediate stations will be provided.

Because of the advantages noted, this method was also chosen for the construction of OKP/break-monitoring equipment/.

According to figure 1, the OKP equipment in the OP/terminal point/ consists of the following: PU/cut-off devices/, IU/measuring device/, RU/recorder/ with a TgA/telegraph apparatus/, and a PrSI/signal notification receiver/. A PU and a PerSI/signal notification transmitter/ have been installed at each OUP/attended repeater station/. The cut-off devices have been switched into the PrKCh/pilot frequency receiver/ outlet. Additionally the PrKCh has a transmission band of several kilohertz, which permits the monitoring of sufficiently short breaks. Thus, the minimum duration of breaks of K-1920 channels along 1056 and 5974 kilohertz linear KCh's amounts to 3 and 1 milliseconds respectively.

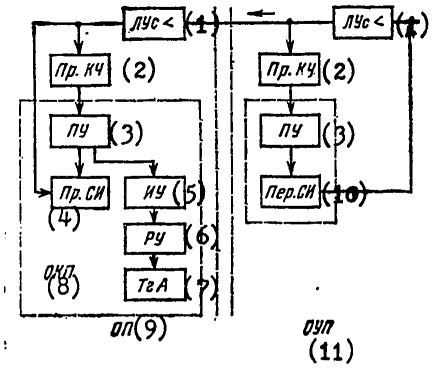

Figure 1.

Key:

1. LUs
2. PrKCh
3. PU
4. PrSI
5. IU
6. RU
7. TgA
8. OKP
9. OP
10. PerSI
11. OUP

FOR OFFICIAL USE ONLY

APPROVED FOR RELEASE: 2007/02/08: CIA-RDP82-00850R000200040044-7

APPROVED FOR RELEASE: 2007/02/08: CIA-RDP82-00850R000200040044-7

The OKP equipment operates in the following way. When breaks occur on any sector, there is a decrease of the signal of the rectified KCh at the outlet of the PrKCh into the OUP and OP, which takes place behind the area of the break's occurrence. This, in turn, causes a triggering of the PU, whose amplitude threshold has been set equal to an 18 decibel decrease of the rated value in the KCh level. The signal from the PU outlet to the OP triggers the IU and begins the process of measuring the number and total duration of the breaks.

The triggering of the PrSI and PerSI of the OUP occurs simultaneously with this. The notification signals are transmitted to the OP side which leads to a determination of the number of the sector where the break has occurred. The transmission is carried on the linear channel in the free gap of the frequencies 1052-1060 kilohertz. The rated frequency of the signals has been selected equal to 1053.6 kilohertz with a transmission level of -26 decibels at the output of the channel LUs/linear amplifier/. These signals are not transmitted continuously but only when breaks occur, i.e., very rarely. The transmission band of the PrSI is about 500 hertz.

Thus, the low transmission level, the narrow bandwidth occupied when transmitting in the free frequency gap and, finally, the infrequency and short duration of the transmission of notification signals--all of this practically frees the operational quality of the linear channel from the influence of the OKP.

After the transmission cycle for the notification signals has ended, the measuring unit stops and then, for several minutes, the process of computing and printing the data with the help of the RU and TgA takes place. This results in the printing and perforating on telegraph tape of the following: the date and time(with an accuracy up to one minute) of the moment when breaks begin, the number and total duration of the breaks, the conventional KCh number, the number of the OUP-OUP sector.

If the breaks exceed 300 milliseconds in duration, then at the end of such breaks(we will call them failures) the RU is triggered and the duration of the failure is recorded. The form for this record is presented below.

Record Form

22	0145	3	1	00	000	0
22	0146	0	1	00	000	3
22	0153	4	1	01	800	0
22	0154	4	1	05	800	9
(1) День	(2) Время	(3) Номер КЧ при начале отказа	(4) Номер участка	(5) Количество перерывов	(6) Длительность перерывов	(7) Номер КЧ при окончании отказа

Key:

1. Day
2. Time
3. KCh number at the start of the failure
4. Sector number
5. Number of breaks
6. Length of the breaks
7. KCh number at the end of the failure

APPROVED FOR RELEASE: 2007/02/08: CIA-RDP82-00850R000200040044-7

APPROVED FOR RELEASE: 2007/02/08: CIA-RDP82-00850R000200040044-7

At the terminal points of the line, the OKP equipment permits the monitoring of four linear channels with two KCh in each and the determining of the area where breaks take place with an accuracy up to the OUP-OUP sector when the number of OUP's is not more than seven. However, both the number of channels and the number of OUP's can be considerably increased with only slight modification to the monitoring equipment.

Research experience on breaks shows that one of the reasons for breaks is the disappearance of the power supply during switches from the main to the reserve power supply soirce of the OUP and OP. It is characteristic for breaks to crop up simultaneously in opposite direction channels. This means that it is sufficient to compare the monitoring data recorded in the opposite OP's to detect such cases.

Another cause of breaks in canals and group channels is the switching from the main to the reserve carrier frequency oscillator. An additional device not shown in figure 1 has been introduced into the OKP equipment to localize the sources of such breaks--this is a unit for monitoring the carrier and pilot frequencies. A selected carrier frequency is monitored periodically with its help. In this case 12 is the maximum number of simultaneously monitored frequencies. The monitoring results are registered by copying readings from machine counters.

Test Results--In 1976 a mock-up of the break-monitoring equipment was installed at a communications center and was switched into the linear channels of three K-1920 mainlines: A, B, and C. The monitoring results have been brought together in table 1. During the processing of the monitoring data an interval of break combination equal to 1 minute was chosen (we note that there are no definitive recommendations concerning the length of the gap of the break combinations and a more accurate definition of it is one of the tasks of further research).

Table 1.

№	Магистраль (1)	Длина тракта, км (5)	Сроки испытаний, год (6)	Продолжительность, месяцев (7)	Число перерывов (8)	Число отказов (9)	$K_п$	$K_о$
1	А	750	1976	8	301	77	50	12,8
2	Б (2)	900	1976	11	30	84	3,2	7,9
3	В (3)	960	1976	11	113	81	10,7	7,6
4	Б (четыре тракта) (4)	4×900	1978	7	68	100	2,6	3,9

Key:

1. Mainline
2. B
3. C
4. B(4 channels)
5. Length of the channel, in kilometers
6. Test periods, by year
7. Duration, in months
8. Number of breaks
9. Number of failures

FOR OFFICIAL USE ONLY

APPROVED FOR RELEASE: 2007/02/08: CIA-RDP82-00850R000200040044-7

APPROVED FOR RELEASE: 2007/02/08: CIA-RDP82-00850R000200040044-7

The coefficients K_n and K_o, denoting respectively the number of breaks and number of failures for one month of observations on 1,000 kilometers of a linear channel, has been introduced to make a comparative analysis of the monitoring results.

The data presented in the table represent a quantitative evaluation, made for the first time, of short-term breaks and failures of K-1920 linear channels during a lengthy observation period. As evident from the table, the channel of mainline A differs from the channels of the other mainlines by the significantly larger number of breaks. The cause of this turned out to be the unreliable operation of the power supply sources. Thus, taking into account the OKP data, it became possible to resolve one of the basic problems, viz., to discover the main, determining source of breaks on mainline activities. Of course, the next step is to develop measures to eliminate the causes of these breaks.

A full complement of monitoring equipment was installed on mainline B in 1978 and it was switched into four channels, i.e., not only to the OP but also to all OUP's. The results obtained during seven months(May-November) of observation have been presented in table 1 for convenience in comparing them with the earlier obtained results. Table 2 contains a distribution of breaks, by cause, for mainline B(1978 tests).

Table 2.

(1) Причина	(2) Число перерывов, %	(3) Число отказов, %
(4) Ремонтно-восстановительные работы	22 (58)	34 (57)
(5) Повреждение источников электропитания	7 (18)	6 (10)
(6) Повреждение оборудования тракта	—	8 (14)
(7) Повреждение кабеля	—	6 (10)
(8) Не выяснен	9 (24)	5 (9)
(9) Всего	38 (100)	59 (100)

Key:

1. Cause
2. Number of breaks, by percentage
3. Number of failures, by percentage
4. Repair and replacement work
5. Damage of power supply sources
6. Damage of channel equipment
7. Damaged cables
8. Unexplained
9. Total

APPROVED FOR RELEASE: 2007/02/08: CIA-RDP82-00850R000200040044-7

APPROVED FOR RELEASE: 2007/02/08: CIA-RDP82-00850R000200040044-7

One can also note the following characteristic cases. Technical personnel, conducting measurements without shutting off communications, were notified by an audible OKP signal when there were breaks caused by a failure of the measuring jack of the linear amplifier. The built-in KCh signalization did not operate at this time because of the short duration of the breaks. This case shows that the rapid notification of personnel can not only speed up the process of localizing the sources of breaks but can also lower the number of breaks due to the failure of measuring instruments and equipment, mistakes and incorrect actions of personnel, etc.

Several cases were observed during the operation of the OKP when, following an increase in the number of short-duration breaks, a total shutdown of channel activities took place. The causes of this were a poor contact in the plug and socket unit and damage to cable insulation. Such cases indicate that one can know beforehand about lengthy failures through monitoring data. However, the use of OKP for this purpose requires some more accumulation of experience and the elaboration of an appropriate methodology.

An Analysis of the Results--From table 1 it is apparent that the channel of mainline B is distinguished by the least number of breaks. This mainline also displays a decrease in the number of breaks and failures in comparison with the earlier obtained data. It can be confirmed that one of the reasons for the favorable dynamics is the introduction of a continuous break-monitoring system.

Table 2 shows that the greater part of breaks(58%) and failures(57%) occurs because of the carrying on of repair and replacement work. One can expect that, thanks to the use of the OKP, and precisely because of the rapid notification of technical personnel, the number of such breaks will be gradually lowered.

An important feature of the results obtained is that more than half of the failures are less than 1-2 minutes long. Such failures are, practically speaking, not detected by technical personnel. This means that with the help of the OKP it is possible to be much more accurate than before in evaluating the reliability of a linear channel and to maintain it within the limits of the standard with failure criteria of 300 milliseconds.

The installation on coaxial cable mainlines of OKP break-monitoring equipment makes it possible to fulfill the aim of eliminating the sources of short-duration breaks and thus increasing the quality of data transmissions, the transmission of newspapers, and voice-frequency telegraphy. OKP is one of the effective instruments of KSUKS/the total system of managing the quality of communications/, which has been intensively introduced on the country's communications networks.

In conclusion the authors express their thanks to the mainline engineers R. M. Yakovleva, A. G. Savel'yeva, M. N. Simakova, L. Duvanova, Yu. I. Mironov, and N. N. Batrayev who participated in the OKP tests.

APPROVED FOR RELEASE: 2007/02/08: CIA-RDP82-00850R000200040044-7

APPROVED FOR RELEASE: 2007/02/08: CIA-RDP82-00850R000200040044-7

BIBLIOGRAPHY

1. Shvartsman, V. O., ed., "Kanaly peredachi dannykh"/Data Transmission Canals/, Moscow, SVYAZ', 1970.

2. Klan, G., "Zuverlassigkeit von Vielkanal-Fernsprechverbindungen(Kurzzeit-Unterbrechungen)", NACHTRICHTEN TECHNISCHE ZEITSCHRIFT, No 9, 1968.

3. "Sistema avtomaticheskoy registratsii pereryvov peredachi pri dlitel'nom nablyudenii KCh pervichnykh, vtorichnykh, i t.d. grupp"/A System for the Automatic Recording of Transmission Breaks during the Lengthy Observation of the KCh of Primary, Secondary, etc. Groups/, Contribution No 141, IK of the 4th MKKTT, Japan, December, 1975.

COPYRIGHT: Izdatel'stvo "Svyaz'", "Elektrosvyaz'," 1979

8524
CSO: 5500

APPROVED FOR RELEASE: 2007/02/08: CIA-RDP82-00850R000200040044-7

APPROVED FOR RELEASE: 2007/02/08: CIA-RDP82-00850R000200040044-7

USSR

UDC 621.395.44

EXPANSION OF THE OPERATING FREQUENCY RANGE OF HIGH CAPACITY BALANCED CABLES FOR ANALOG TRANSMISSION SYSTEMS

Moscow ELEKTROSVYAZ' in Russian No 10, 1979 pp 12-16

/Article by B. M. Fayerovich and Ye. T. Khvostovitskiy/

/Text/ Balanced high-frequency cables with various numbers of pairs(1x4, 4x4, 7x4, etc.) and various modifications(MKSB, MKSAShp, MKSSShp, MKB) have been widely disseminated in our country. Yet balanced cables are used ineffectively in comparison with the coaxial cables on which 300, 1920, and 3600 canal transmission systems operate. Some 60 TCh(tone frequency) canals are arranged along each pair of a balanced cable which amounts to a total of 480 canals for a cable with a 4x4 capacity, and 840 canals for a 7x4 cable. Therefore the task of increasing the traffic carrying capacity of balanced cables has great national economic importance.

Specifically, these questions have been worked up as suitable for analog systems. The possibility of arranging a 300-canal system along one pair of MKPV 1x4x1.2[2] cable has been studied and verified experimentally by Mezhgorsvyaz'stroy/All-Union State Trust for the Construction of Long-Distance Wire Communications Structures/. TsNIIS/Central Scientific Research Institute of Communications/ is developing a 1020-canal system for one pair of 4x4 and 7x4[3] cable. These solutions are progressive, but not optimal, so long as the traffic carrying capacity of the rest of the pairs of the cable is not increased.

One can also increase the traffic carrying capacity of balanced VCh/high frequency/ cables by arranging TsSP/digital transmission systems/ on them. However, at the same time, the effectiveness of using circuits is inadequate when compared with analog systems. Thus, a secondary TsSP IKM-120 with a regenerated section length of five kilometers permits the organization of 120 TCh channels[4] along a balanced pair, and a K-300 analog system with a repeater section length of six kilometers permits 300 TCh canals.

Thus, the optimum solution is to set up analog transmission systems with a number of canals on each pair of balanced cable, approaching the number of canals set up on the coaxial pair.

FOR OFFICIAL USE ONLY

APPROVED FOR RELEASE: 2007/02/08: CIA-RDP82-00850R000200040044-7

APPROVED FOR RELEASE: 2007/02/08: CIA-RDP82-00850R000200040044-7

Up to the present time it was not possible because of interference between circuits to set up with more than 60 TCh canals(i.e., in the frequency spectrum above 252 kilohertz) over all pairs of transmission system balanced cable. In recent years a method has been worked out for increasing the inter-protection f circuits on OUP-OUP[1] /attended repeater station to attended repeater station/ sections which permits the solution of the problem of significantly increasing the traffic carrying capacity of the balanced cables of communications lines. For a practical solution to this problem it is necessary to carry out a number of studies in the different frequency ranges and based on manufactured coaxial cable equipment to create a transmission system over high-capacity balanced cables. Such a system can be, for example, the K-300SM system which was developed by specialists of the USSR Ministry of Communications.

Interference Between Circuits on OUP-OUP Sections--Between two balanced cable circuits equipped with repeaters(figure 1), there is interference characterized by complex communications at the end of the OUP-OUP section. These communications are defined by the expression

$$Y_{\text{оуп}} = \sum_{k=0}^{N} y_{\substack{1-2\,k\\(2-1)}} \times$$
$$\times e^{\pm\left[\sum_{i=k}^{N-1}(S_{2i}-S_{1i})-(\gamma_2-\gamma_1)\sum_{i=k+1}^{N} l_i\right]}, \quad (1)$$

where $\gamma_1=\alpha_1+i\beta_1$, $\gamma_2=\alpha_2+i\beta_2$ are the constant transmissions of the first and second cable circuits; l_i is the length of the i NUP-NUP /uncontrolled repeater station to uncontrolled repeater station/ section; $S_{1i}=s_{1i}+i\varphi_{1i}$, $S_{2i}=s_{2i}+i\varphi_{2i}$ are the coefficients of the gains of the repeaters of the first and second systems of the i NUP; $y_{\substack{1-2\,k\\(2-1)}}$ is the complex communications between circuits 1 and 2(2 and 1) of the k NUP-NUP section during the feeding of the generator in the first(second) system; N is the number of NUP-NUP sections on the OUP-OUP sector.

If two interfering cable circuits are located within one quad, then $\gamma_1=\gamma_2$ * $S_{1i}=S_{2i}$. Moreover

$$Y_{\text{оуп}_{\substack{1-2\\(2-1)}}} = \sum_{k=0}^{N} y_{\substack{1-2\,k\\(2-1)}}. \quad (2)$$

Different cable quads have various lays for ensuring minimum interference between the circuits from different quads. The smaller the lays, the greater the length of the circuit per unit of cable length and, consequently, the greater the γ of this circuit. In the case of interference to the circuits from the different quads $\gamma_1 \neq \gamma_2$ and correspondingly $S_{1i} \neq S_{2i}$. From (1) it follows that the complex communications of each repeater section at the end of the OUP-OUP sector are changed by module and receive an additional phase shift, while these changes in direct(1-2) and reverse (2-1) combinations of the influencing circuits have an opposite character.

APPROVED FOR RELEASE: 2007/02/08: CIA-RDP82-00850R000200040044-7

APPROVED FOR RELEASE: 2007/02/08: CIA-RDP82-00850R000200040044-7

Figure 2a and b shows time graphs of intra and inter-quad KhKS/characteristics of complex communications/ at the end of the OUP-OUP sectors measured in the 12-252 kilohertz frequency range. Very apparent are the effects determining the complexity of the KhKS: rearrangements(the time curves 1-2 and 2-1 are not identical), looping(the time curves have large-diameter loops), and left looping(time curve 2-1 of the inter-quad combination of influences has a counter clockwise direction during a frequency increase.

Causes Limiting the Frequency Range Utilized When Balancing Cable--Cable balancing on each NUP-NUP section is carried out(see figure 1) to ensure the necessary protection from interference. It is accomplished thusly: by the selection of circuit crossing operators within quads at three points (couplings) of the NUP-NUP section to eliminate the effects of shifting and looping in intra-quad influence combinations; by the inclusion of concentrated balancing elements--condensers or two-terminal networks from the consecutively combined elements R and C--for balancing divided two-terminal pair networks of interference between two circuits; the inclusion of concentrated balancing elements of intra-quad influence combinations simultaneously at two points of the NUP-NUP sector in cases of shifting and left looping.

From (1) and (2) it follows that the KhKS between the cable circuits on the NUP-NUP section is considerably simpler than the KhKS between the channels on the OUP-OUP section determined by the sum of the complex communications of all NUP-NUP sectors. In the frequency range up to 252 kilohertz, the balancing methods which have been listed sufficiently provide the required protection standards except in cases of low quality cable packing. Figure 3a and b depict the typical KhKS between two circuits of a NUP-NUP sector up to and after the selection of crossing operators as well as the time curve for the condition of a balanced circuit RC(b).

The complexity of the KhKS between the cable circuits grows with an increase in the frequency range. On the NUP-NUP sector the KhKS become similar to the KhKS shown in figure 2 and the balancing will cease to be effective.

A method to increase the protection between circuits on an OUP-OUP section is to switch a quadripole into the interfering circuits at the end of the section, for example, in the receiving OUP. A part of the influencing signal is drawn through it into the circuit exposed to the influence, into a reverse phase with the interference and compensates for it(figure 4). The effect of shifting is overcome by the use of OU/unidirectional gear/, switched in series with compensating quadripoles or with KPS/anti-communications networks/ (figure 5), and the effect of looping is overcome by using complex KPS arrangements containing, besides the RC elements, four-radial star circuits with inductances(figure 6), elements of which are determined by computer calculations through a specially developed program(the time curve of the conduction of the link RLS has been presented in figure 7). The effect of left looping is overcome by switching the KPS into a combination of influences with a given effect on the transmitting OUP.

FOR OFFICIAL USE ONLY

APPROVED FOR RELEASE: 2007/02/08: CIA-RDP82-00850R000200040044-7

APPROVED FOR RELEASE: 2007/02/08: CIA-RDP82-00850R000200040044-7

The availability of solutions to overcome all three effects which inhibit a lessening of interferences between circuits, permits us to approach in a new way the task of providing the necessary protection from linear jumps and, specifically, it raises the question concerning the failure of cable balancing on repeater sections. Possibilities are also unfolding to compensate for interference on frequencies which correspond to the operating range of transmission systems over coaxial cables.

Basic Trends in Research--The following problems arise when the frequency range is significantly broadened:

1. The influence of spurious capacitance grows(in figure 8 the spurious capacitance 1 пФ at frequencies of 1 and 10 megahertz respectively exerts 10 and 100 times greater influence in comparison with its influence at a frequency of 100 kilohertz), which creates considerable difficulties both during KPS synthesis and also during KhKS measurements. As a possible solution, one can suggest a consecutive switching in with the KPS of the attenuator to increase the conductance of the compensating elements, thereby lowering the influence of the spurious capacitances. At the same time we obtain the transmission factor $K = K_y \cdot K_{kps}$ where the transmission factor of the attenuator is determined by the ratio $|K_y \omega_в| < 1$; and $\omega_в$ is the upper broadcast frequency.

2. The difference of the circuit phases from the various cable quads grows with an increase of frequency. Specifically, for MKS 4x4 cable of the Moskabel'/Moscow Cable/ Plant, this difference according to measurement results amounts to 8f degrees per kilometer. Moreover on an OUP-OUP section 200 kilometers long, the difference of the circuit phases amounts to 2400 degrees, i.e., 6.5 revolutions of the time curve at a frequency up to 1.5 megahertz, and 13,800 degrees or 38 revolutions of the KhKS time curve at a frequency up to 8.6 megahertz. To compensate for one loop of the time curve, it is necessary to have not less than one RLS link, and very complex KPS diagrams are required in all intra-quad combinations. One solution to the problem is the levelling off of continual circuit propagation by mixing the cable quads.

3. When switching on of KPS at the end of the OUP-OUP section, the protection between circuits is determined by the expression

$$A_э = \ln \frac{8}{|(Y_{оуп} - Y_{кпс})\, Z_н|}.$$

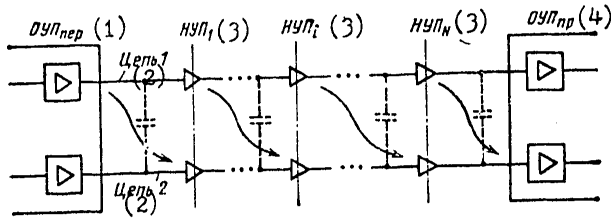

Figure 1.

Key:

1. Transmitting OUP
2. Circuit
3. NUP
4. Receiving OUP

APPROVED FOR RELEASE: 2007/02/08: CIA-RDP82-00850R000200040044-7

APPROVED FOR RELEASE: 2007/02/08: CIA-RDP82-00850R000200040044-7

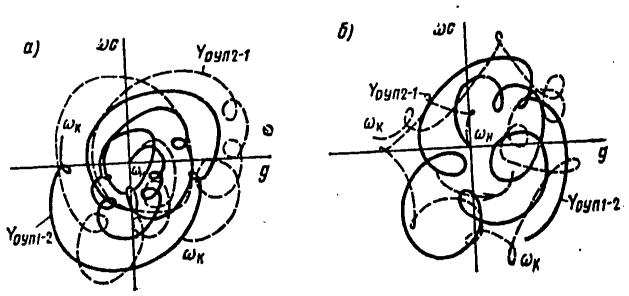

Figure 2.

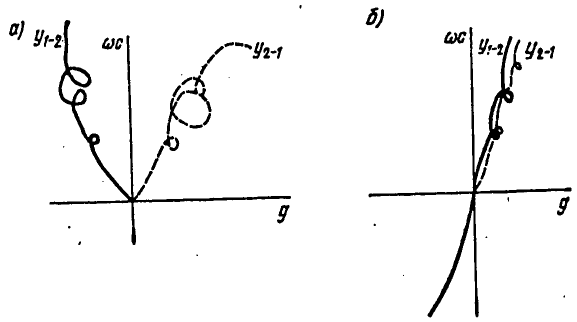

Figure 3.

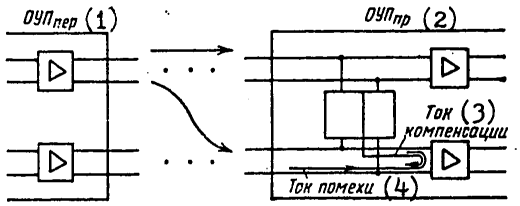

Figure 4,

Key:
1. Transmitting OUP
2. Receiving OUP
3. Balancing current
4. Noise current

FOR OFFICIAL USE ONLY

APPROVED FOR RELEASE: 2007/02/08: CIA-RDP82-00850R000200040044-7

APPROVED FOR RELEASE: 2007/02/08: CIA-RDP82-00850R000200040044-7

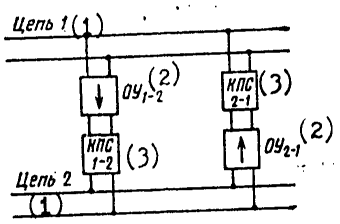

Figure 5.

Key:
1. Circuit
2. OU
3. KPS

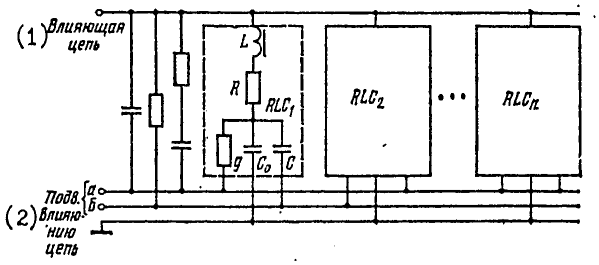

Figure 6.

Key:
1. Acting circuit
2. Under the acting circuit

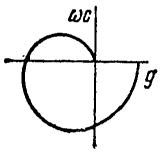

Figure 7.

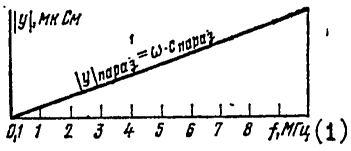

Figure 8.

Key:
1. Megahertz

APPROVED FOR RELEASE: 2007/02/08: CIA-RDP82-00850R000200040044-7

APPROVED FOR RELEASE: 2007/02/08: CIA-RDP82-00850R000200040044-7

During seasonal ground temperature fluctuations, because of errors introduced into the thermal APU/automatic gain control/ of the parallel system repeaters, Y_{oup} will be changed to the value

$$\Delta Y_{\text{оуп}} = \sum_{k=1}^{N} y_{\substack{1-2k \\ (2-1)}} \times$$
$$\times \left[\sum_{i=k}^{N} (\Delta s_{1i} + \Delta s_{2i}) + i(\Delta \varphi_{1i} + \Delta \varphi_{2i}) \right].$$

The number of repeaters on an OUP-OUP section grows with an increase in the frequency range. Although Δs and $\Delta\varphi$ of each repeater are very small, yet, with a large number of boosters, the total change of Δs and $\Delta\varphi$ can lead to a noticeable change of Y_{oup} and correspondingly A_3 as a whole. To weaken the given effect it is advisable for one either to take special measures to decrease Δs and $\Delta\varphi$ (for example, by the selection of thermoresistances, installed in one block of the thermal ARU), or to decrease the value of complex communications on each NUP-NUP sector by installing anti-communication simplified circuit devices in the NUP. Moreover it is necessary to determine and standardize the values Y_{oup} and y_k, providing sufficient stability of protection during the use of simple anti-communications systems, distributed along the length of the OUP-OUP section, and complex anti-communications at the end of the section.

Besides the basic problems which have been stated for the specified wide frequency ranges, it is necessary to develop a computer program of KPS elements, and also to create a unidirectional device, a UPS/anti-communication device/, a device for KhKS measurements, etc. The solution of the problems listed, and also the clearing up of the technical and economic side (the complexity of compensating devices, their cost, the complexity and cost of work on providing protection) permits the installation of utilization thresholds of balanced cables for analog transmission systems during the existing normalization of interference in the TCh/tone frequency/ canals.

The Technical and Economic Basis--The arrangement over existing balanced cables of 300-canal systems instead of the 60-canal systems which have been used permits a fivefold increase in the network's traffic carrying capacity. Moreover it will become possible to organize 2400 TCh canals along a 4x4 cable and 3600 canals along a 7x4 cable(without using a central quad), in separate directions, because of the packing of the existing balanced cable--new coaxial lines will not have to be laid(the cost of 1000 kilometers of coaxial cable including the laying and installation amounts to about six million rubles for MKT-4 cable and eight million rubles for KMB-4 cable). If the results of studies show that it is possible to arrange 1920-canal systems(i.e., 15,360 TCh canals over a 4x4 cable) along balanced cable, then the entire existing network will be sufficient within the next few years with a number of canals for the transmission of various data, including television, without additional expenditures for new cable.

FOR OFFICIAL USE ONLY

APPROVED FOR RELEASE: 2007/02/08: CIA-RDP82-00850R000200040044-7

APPROVED FOR RELEASE: 2007/02/08: CIA-RDP82-00850R000200040044-7

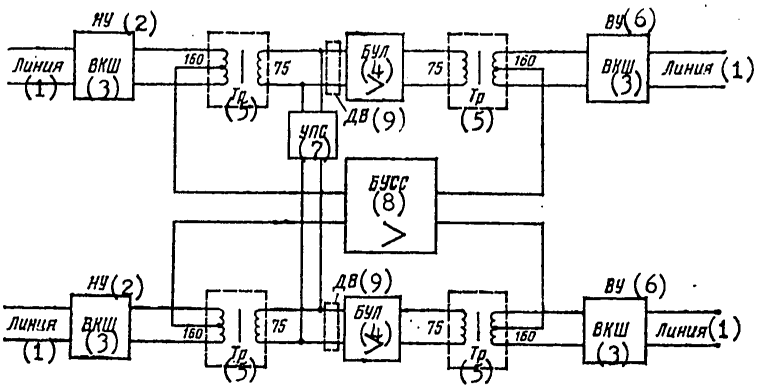

Figure 9.

Key:

1. Line
2. NU
3. VKSh
4. BUL
5. TR
6. VU
7. UPS
8. BUSS
9. DV

Practical Steps Toward the Creation of Equipment--To increase the quality of communications cable lines, the SKL GTsUMS/Cable Line Service of the Main Control Center of Interurban Communications of the USSR Ministry of Communications/ is preparing an experiment on organizing eight 300-canal systems along a balanced MKSASh$_p$ 4x4x1.2 cable with the use of K-300 series semiconductor equipment. To change from balanced cable to equipment intended for coaxial cable, additional 160/75 matching transformers and equalizers(DV) are required. They serve to eliminate the difference between the AChKh /amplitude frequency characteristics/ of balanced and coaxial circuits. A block diagram of the passage of circuits into the NUP has been shown in figure 9. The repeater equipment of the new K-300SM system(balanced, large-capacity), installed in the NUP, can be mounted in the shape of a unified brace for eight VCh circuits, a communications servicing circuit and a telemechanics circuit. The intention is to arrange the brace in a standard horizontal shortened K-60P tank.

APPROVED FOR RELEASE: 2007/02/08: CIA-RDP82-00850R000200040044-7

APPROVED FOR RELEASE: 2007/02/08: CIA-RDP82-00850R000200040044-7

The new K-300SM system can be rather quickly checked out on an experimental section and, within the next few years, it will be introduced on the main cable lines of the country.

BIBLIOGRAPHY

1. Fayerovich, B. M., "Povysheniye zashchishchennosti na uchastkakh OUP-OUP"/Increasing the Protection on OUP-OUP Sectors/, Moscow, SVYAZ', 1976.

2. Kononov, A. G., Rombro, V. S., Farber, Yu. D.,"Sistema K-300 dlya simmetrichnykh kabeley 1x4x1.2"/The K-300 System for 1x4x1.2 Balanced Cables/, ELEKTROSVYAZ', No 4, 1978.

3. Kim, L. T., Rapoport, E. Z., "Sistema peredachi K-1020S"/The K-1020S Transmission System/, ELEKTROSVYAZ', No 8, 1979.

4. Lopushnyan, Yu. G. and others, "Apparatura vtorichnoy tsifrovoy sistemy peredachi IKM-120"/Equipment of the IKM-120 Secondary Digital Transmission System/, ELEKTROSVYAZ', No 12, 1977.

COPYRIGHT: Izdatel'stvo "Svyaz'', "Elektrosvyaz'," 1979

8524
CSO: 5500

END

APPROVED FOR RELEASE: 2007/02/08: CIA-RDP82-00850R000200040044-7